



Kolomvatsos, K. and Anagnostopoulos, C. (2019) Multi-criteria optimal task allocation at the edge. *Future Generation Computer Systems*, 93, pp. 358-372.  
(doi:[10.1016/j.future.2018.10.051](https://doi.org/10.1016/j.future.2018.10.051))

There may be differences between this version and the published version. You are advised to consult the publisher's version if you wish to cite from it.

<http://eprints.gla.ac.uk/172893/>

Deposited on: 6 November 2018

Enlighten – Research publications by members of the University of Glasgow  
<http://eprints.gla.ac.uk>

# Multi-criteria Optimal Task Allocation at the Edge

Kostas Kolomvatsos, Christos Anagnostopoulos

*School of Computing Science, University of Glasgow  
Glasgow, UK*

*e-mails: {Kostas.Kolomvatsos, Christos.Anagnostopoulos}@glasgow.ac.uk*

---

## Abstract

In Internet of Things (IoT), numerous nodes produce huge volumes of data that are subject of various processing tasks. Tasks execution on top of the collected data can be realized either at the edge of the network or at the Fog/Cloud. Their management at the network edge may limit the required time for concluding responses and return the final outcome/analytics to end-users or applications. IoT nodes, due to their limited computational and resource capabilities, can execute a limited number of tasks over the collected contextual data. A challenging decision is related to which tasks IoT nodes should execute locally. Each node should carefully select such tasks to maximize the performance based on the current contextual information, e.g., tasks' characteristics, nodes' load and energy capacity. In this paper, we propose an intelligent decision making scheme for selecting the tasks that will be locally executed. The remaining tasks will be transferred to peer nodes in the network or the Fog/Cloud. Our focus is to limit the time required for initiating the execution of each task by introducing a two-step decision process. The first step is to decide whether a task can be executed locally; if not, the second step involves the sophisticated selection of the most appropriate peer to allocate it. When, in the entire network, no node is capable of executing the task, it is, then, sent to the Fog/Cloud facing the maximum latency. We comprehensively evaluate the proposed scheme demonstrating its applicability and optimality at the network edge.

*Keywords:* Edge-centric computing, task allocation, multi-criteria decision making

---

## 1. Introduction

The Internet of Things (IoT) gives the opportunity for the creation of intelligent applications on top of numerous computing, sensing, and actuation devices. Devices are interconnected to communicate while they collect data from their environment and process them becoming knowledge producers. Knowledge may have the form of a response in analytics queries (predictive and inferential analytics) defined by end-users or applications [35], or they may be the result of more complicated tasks. Legacy systems adopt the Cloud infrastructure where various services' models are available. However, large-scale data centers, present in Cloud, are centralized systems which implies a large average separation between devices and Cloud. This, in turn, increases the average network latency and jitter negatively affecting delay sensitive, real-time applications [40].

For alleviating the problem of delay, Edge Computing (EC) [38] is coming into scene. In EC, numerous human-controlled devices form the network edge like tablets, smart-phones, sensors or nano data-centers [16]. Edge-centric computing aims at a distributed model that interconnects heterogeneous resources controlled by various nodes to the Fog and, accordingly, to the Cloud. In EC, we can deploy Cloud-like capabilities in the devices to make them able to process the collected data. Hence, we minimize the required time for initiating tasks processing and acquiring responses. Fog Computing (FC) is the next step, one hop away for the data production and the aforementioned pre-processing model. In FC, nodes communicate with cloudlets, and cloudlets communicate with Cloud to realize the data processing and analytics tasks. Both EC and FC aim to keep processing tasks close to the nodes, thus, the sources of contextual data to limit the latency in the provision of responses. Recent advances in the field involve the adoption of light weight virtualization techniques on top of the available heterogeneous devices present at the EC [29]. The orchestration of the devices could be realized through containers or unikernels facilitating the packaging of the provided services [33]. A comprehensive performance evaluation that aims to show the strengths and weaknesses of several low-power devices when handling container-virtualized instances is presented in [28] while their suitability is reviewed in [34]. Other recent approaches incorporate P2P control protocols for the exchange of service provisioning information between various FC nodes and their coordination [39].

For supporting IoT applications, edge nodes should perform/execute a

38 set of tasks. Tasks are generated, possibly, at high rates and should be  
 39 concluded immediately in terms of allocation and execution. In the rele-  
 40 vant literature (see next Section), task allocation and scheduling originates  
 41 in the management of a group of nodes. The allocation is, then, adopted  
 42 to determine the assignment of each task to a node while scheduling mainly  
 43 aims to the sequence of the execution for each task. The challenges are to  
 44 **(C1)** maximize the performance and **(C2)** minimize the energy consump-  
 45 tion, thus, maximizing the lifetime of the network. Multiple research efforts  
 46 deal with centralized approaches, thus, the allocation and scheduling models  
 47 suffer from the drawbacks reported in the literature for Cloud computing.  
 48 In this paper, we build on the *autonomous* nature of nodes and propose  
 49 a distributed scheme for *pushing* the local optimum allocation of incoming  
 50 tasks from centralized decision making to the network edge. In contrast to  
 51 other research efforts elaborated in Section 2, we consider that each task  
 52 can be **(i)** executed in an edge node itself, or **(ii)** executed in a group of  
 53 peer/neighbors nodes, or **(iii)** delegated to the Fog/Cloud. Due to energy  
 54 and computational constraints, each node can afford a limited number of  
 55 tasks; it should select those that *maximize* its performance while meeting  
 56 certain resource constraints. The rationale behind our scheme is that we  
 57 distinguish two conditional decisions on an edge node: the first decision is  
 58 related to whether a task *can be executed locally*. The second decision is  
 59 related to whether the task *can be executed in the group of peers* or in  
 60 the Fog/Cloud conditioned on the result of the former decision. The aim is to  
 61 *optimally* decide the execution of tasks starting from the node itself to min-  
 62 imize the time for initiating the execution. The first decision is achieved by  
 63 a classification model derived from an  $k$ -Nearest Neighbor Classifier ( $k$ NNC)  
 64 [20]. The conditional second decision is obtained by adopting the utility the-  
 65 ory [17]. For both decisions, we aim to find the closeness of the incoming  
 66 tasks with (in a sequential order): (i) the training set adopted to indicate  
 67 which tasks should be executed locally based on a set of constraints; (ii) the  
 68 characteristics of the peers in the network. Both decisions are made over  
 69 contextual information related to the status/context of the node, e.g., cur-  
 70 rent load, remaining resources, collected data distribution, and every task's  
 71 characteristics, e.g., priority, execution requirements.

72 The paper is organized as follows: Section 2 reports on the related work  
 73 and how our mechanism departs from it discussing the key contribution  
 74 points. Section 3 presents the problem of pushing the task allocation to  
 75 the edge and the decision making methodology. In Section 4, we describe

the proposed in-network centric approach while in Section 5, we provide an analysis for the short- and long-term load of nodes. In Section 6, we present the experimental evaluation of the proposed scheme and Section 7 concludes the paper discussing our future research plans.

## 2. Related Work & Contribution

Tasks allocation and scheduling are important research subjects in multiple domains. Both subjects have a significant impact in the IoT and EC as nodes have limited computational capabilities while being restricted by various energy constraints. Hence, nodes should carefully select the tasks that they will execute locally making imperative the need for applying intelligent techniques for tasks scheduling. In any case, nodes should take into consideration tasks' specific characteristics in combination with their current status for any decision making. Cloud serves as the intermediate between IoT devices and applications exhibiting a vast infrastructure where increased computational (possibly virtualised) capabilities are available for processing. EC provides the necessary framework for hosting and executing tasks with the minimum delay/latency. Smart gateways and micro-data centers are adopted to facilitate the task processing [1], [19]. A widely studied research subject is task scheduling in Wireless Sensor Networks (WSNs). Task mapping and scheduling should take into consideration energy constraints to secure an efficient execution [48], [6]. A task pre-processor and a scheduler can be responsible for the final allocation. The pre-processor tries to identify the energy requirements of the incoming tasks and, based on energy monitoring activities, decides on the final scheduling. Another approach is to study a fair energy balance among sensors while minimizing the delay using a market-based architecture [12]. Nodes are modeled as sellers communicating a deployment price for a task to the consumer. Taking into consideration the defined constraints, nodes may cooperate to conclude the final allocation of tasks [2]. Example algorithms involve task clustering and node assignment mechanisms based on task duplication and migration schemes. In any case, the aim is to minimize the execution time, thus, to deliver the final response in limited time [10]. A model that could be adopted for such purposes is to cluster the network and build intra-cluster and inter-cluster scheduling relations. An Integer Linear Programming (ILP) formulation and a 3-phase heuristic are also adopted to solve the task allocation problem in [57]. Each sensor node is equipped with discrete Dynamic Voltage Scaling (DVS) while

the time and energy costs of both computation and communication activities are considered. In [56], the authors propose a modified version of binary Particle Swarm Optimization (PSO). The method adopts a different transfer function, a new position updating procedure and mutation for the task allocation problem. Another PSO-based solution is presented in [37] which allocates tasks into a number of robots trying to decrease the communication cost. In [22], the authors present a task allocation mechanism of a dynamic alliance that is based on a Genetic Algorithm to acquire the balance between energy consumption and accuracy. In [9], the authors discuss three algorithms to solve the task allocation problem: a centralized, an auction-based, and a distributed algorithm. The distributed algorithm adopts a spanning tree over the static sensors to assign tasks.

A set of sub-tasks may consist of a more generic task. The efficient combination and execution of sub-tasks will lead to the efficient completion of the initial, more generic, task. A scheduling algorithm for a set of sub-tasks is proposed in [51]. The aim is to assign each sub-task into the available nodes for maximizing the performance. Zenith [54] proposes a methodology for resource allocation in a set of small-scale micro-data centers that represent an ad-hoc and distributed collection of a computing infrastructure. Zenith allows service providers to establish resource sharing contracts with the edge infrastructure.

Task scheduling heavily depends on the application domain. IoT and Cloud define different requirements due to their different nature. Cloud mainly offers the available services on demand, while the IoT may involve applications where nodes push their data and knowledge into the network. A review on scheduling algorithms that fit on both the Cloud and the IoT is presented in [41]. In [35], the authors propose a model for data distribution over IoT devices. The model aims to eliminate bandwidth and storage constraints. Simulated annealing is also adopted to solve the problem of scheduling while optimization techniques can be used on top of the load of tasks in Cloud applications [30]. The model tries to build on the parallelization of allocating various tasks in a multi-cloud system. Another task allocation scheme for Cloud is presented in [58]. The provided model takes into consideration both task and nodes diversity. Workloads are clustered into different classes with the same characteristics through the adoption of the k-means algorithm. In [25], the authors propose a Quality of Service (QoS) aware resource scheduling algorithm adopting a PSO model to derive the final scheduling. The aim is to reduce the required time for deciding

150 the final allocation and ensure the load balancing towards the maximization  
 151 of the performance. Finally, JarvSis is proposed as a distributed scheduler  
 152 capable of automating the execution of multiple heterogeneous tasks in IoT  
 153 [5]. Through JarvSis, developers can easily configure and deploy hierarchies  
 154 of control tasks.

155 Recently, research community focuses on the management of virtualized  
 156 resources and their combination to perform processing at the edge of the net-  
 157 work. Some efforts incorporate algorithms for the allocation of the processing  
 158 tasks to the available nodes. For instance, in [46], the authors propose a novel  
 159 workflow-like service request scheme and a dynamic algorithm for allocating  
 160 the virtualized resources to multiple processing points. The aim is to map  
 161 the requests defined in a workflow format to the services offered by the edge  
 162 computing. The provided simulations reveal the minimum latency and an  
 163 efficient behavior when uploading the involved virtualized resources. In ad-  
 164 dition, the research effort presented in [47] aims at proposing a model for  
 165 the management of Cloud-of-Things and Edge Computing (CoTEC) traffic  
 166 in multi-domain networks. In this effort, the proposed scheme incorporates  
 167 traditional multi-topology routing and introduces a number of programmable  
 168 nodes that can be configured to ease the ongoing traffic. Routing tasks are  
 169 allocated to the available nodes while the provided results show a lower ex-  
 170 ecution time and a better quality of service compared to a model that does  
 171 not adopt the proposed algorithm.

172 Studying other relevant efforts in the field, we observe that the majority  
 173 of them focus on the WSNs domain. Hence, the main attention is paid on  
 174 energy constraints when finalizing the allocation of tasks. In addition, they  
 175 also focus on eliminating the communication overhead towards the reduction  
 176 of messaging to lower the transmission collisions. They are, usually, *central-*  
 177 *ized* approaches, i.e., a central entity decides on the final allocation based  
 178 on the currently available contextual information. This inevitably conveys  
 179 the disadvantages of any centralized system, i.e., increased communication  
 180 overhead and a single point failure. The central entity can also decide to  
 181 transfer the data to the node where each task will be executed (with the use  
 182 of migration algorithms). In general, migration techniques focus on ‘univari-  
 183 ate’ contextual information. This means that the final decision is delivered  
 184 taking into consideration only a single parameter/perspective, e.g., energy,  
 185 transmission requirements, topology of the network. More importantly, data  
 186 migration techniques suffer from the increased migration cost especially at  
 187 the network edge due to the increased amount of data ‘circulated’ in the net-

188 work. To the best of our knowledge, our scheme is one of the first attempts  
189 that departs from the centralized task allocation intelligence and focuses on  
190 a distributed, local ‘multivariate’ scenario where the intelligence is pushed  
191 to the edge of the network. The final decision is locally made taking into  
192 account multiple parameters, e.g., the current load of nodes, their speed of  
193 processing, the communication cost, and the remaining resources. That is,  
194 our scheme casts as a local multi-criteria optimization mechanism for deliver-  
195 ing the best decision. Apart from that, we further take into consideration the  
196 data collected at each node without adopting any data migration solutions,  
197 thus, avoiding redundant communication overhead. The proposed sequential  
198 decision making scheme aims to eliminate the initiation time of a task giving  
199 priority to the local execution, i.e., to the node where each task is initially  
200 reported.

201 Our model can be also combined with other schemes recently proposed  
202 for the management of tasks at the edge of the network. For instance, the  
203 virtualized resources allocation for processing [46] or the deployment of net-  
204 work services into a set of programmable router nodes [47] could be the first  
205 step before the execution of our scheme. Such efforts (i.e., [46], [47]) focus  
206 on an allocation based on a ‘global’ view on the available processing points  
207 / nodes deciding over the information available for the present nodes. This  
208 information is related to the network performance. Our scheme could consist  
209 of the second step where every node receiving a task could decide if it has  
210 the resources and the data to process the task locally. Hence, in this second  
211 step, we have the nodes deciding based on the ‘local’ view on their status  
212 and their peers. Actually, the output of the algorithms like those provided in  
213 [46] & [47] could be the starting point for our model triggering the efficient  
214 management of the incoming tasks.

215 The following list summarizes the contributions of our paper:

- 216 • we provide a distributed, ‘multivariate’ decision making mechanism for  
217 the optimal allocation of tasks;
- 218 • our model ‘reasons’ over the status and the data present in each au-  
219 tonomous node;
- 220 • our mechanism does not require the migration of data to become the  
221 subject of tasks’ execution, thus, we avoid the redundant communica-  
222 tion overhead in the network;



- 223 • the proposed mechanism decides based on the ‘local’ view of the status  
224 of each node;
- 225 • we provide a large set of simulations adopting real and synthetic data  
226 together with a comparative assessment with other models in the do-  
227 main.

### 228 3. High Level Description of the Proposed Scheme

229 We consider a set of IoT nodes, i.e.,  $\mathcal{N} = \{n_1, n_2, \dots, n_{|\mathcal{N}|}\}$  responsi-  
230 ble to ‘observe’ their environment and collect contextual data. On top of  
231 the collected data, nodes can execute a set of (simple) processing tasks. A  
232 task stream  $\mathcal{T}_i$  reported to node  $n_i$  is defined by a series of ordered tuples  
233  $\langle t, T_{it}, \mathcal{C}_{it} \rangle$ , where  $t$  is the time-stamp of the task  $T_{it}$  and  $\mathcal{C}_{it}$  is the set of  
234 constraints for  $T_{it}$ . The processing of each task corresponds to a result that  
235 is delivered to end users or applications. We consider that every task is ac-  
236 companied by a set of constraints  $\mathcal{C} = \{c_1, c_2, \dots, c_{|\mathcal{C}|}\}$ . For instance, let  
237  $\mathcal{C} = \{\textit{latency}, \textit{lifetime}\}$  be the set of constraints and  $\mathcal{C}_{it} = \{2.0, 15\}$  is their  
238 realization reported for  $T_{it}$  at some time instance  $t$ . When no constraints are  
239 present, then  $\mathcal{C}_{it} = \emptyset$ . Among the characteristics/constraints of a task, in  
240 this paper, we focus on its priority and complexity. Such parameters depict  
241 two significant aspects of a task execution process, i.e., an indication of the  
242 immediate initiation of its execution (priority) and the time and resources  
243 required for the execution (complexity).

244 Constraints can be in any form, however, a methodology that matches  
245 them to nodes’ characteristics is necessary. We could consider constraints  
246 related to libraries that should be adopted by nodes when executing a task,  
247 we could involve intervals or non-linear relations and match them with the  
248 specific characteristics of each node. Constraints can be incorporated in an  
249 ‘aggregation’ function that will result a subset of them that will be taken  
250 into consideration in the final processing. An aggregation function could in-  
251 corporate the strategy that we want to adopt when deciding to execute each  
252 incoming task. For instance, the involvement of specific libraries or non-  
253 linear relations between constraints may increase the execution complexity  
254 of a task with specific consequences in the decision making. The aforemen-  
255 tioned approach is part of our future research plans. In Figure 1, we show  
256 an example environment with  $|\mathcal{N}| = 4$  nodes. After the reception of task  
257 through  $\mathcal{T}_i$ ,  $n_i$  should decide if it should execute it locally or transfer it to its

258 peers/Fog/Cloud. Specifically,  $n_i$  should sequentially decide on the following  
 259 actions: **Action 1.** Execute  $T_{it}$  locally; **Action 2.** Send  $T_{it}$  for execution  
 260 to one of the peers present in the same local network; **Action 3.** Send  $T_{it}$   
 261 to be executed in the Fog/Cloud. Actually, these actions could be seen as  
 262 the result of two sequential decisions, i.e, **D1.** Decide if  $n_i$  can execute  $T_{it}$ ;  
 263 **D2.** If not, decide if there is a peer node to ‘host’  $T_{it}$ . Actions 2 and 3 are  
 264 examined conditioned to the decision for Action 1.

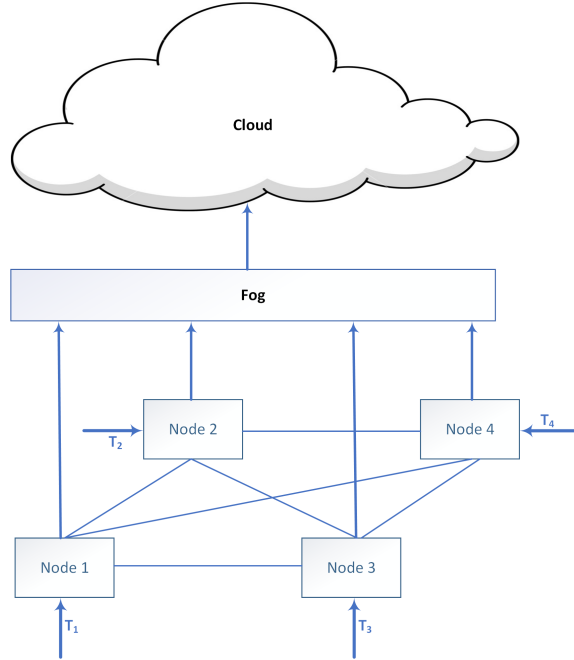


Figure 1: An example of an edge-network architecture with task flows among edge nodes.

265 Locally,  $n_i$  after the reception of  $T_{it}$ , it concludes, based on its current sta-  
 266 tus and  $T_{it}$ 's requirements a *Task Requirements Tuple* (TRT) i.e.,  $\langle l_t, r_t, z_t, b_t \rangle$ ,  
 267 where  $l_t$  is the current load,  $r_t$  is the remaining resources,  $z_t$  is the priority of  
 268 the task and  $b_t$  is the complexity of the task;  $l_t, r_t, z_t, b_t \in [0, 1]$ . In this paper,  
 269 we rely on the priority and complexity of a task a representative character-  
 270 istics/constraints for indicating the time and resources requirements that  
 271 should be met when allocating tasks to the available nodes. Without loss of  
 272 generality, we consider that  $l_t$  and  $r_t$  represent, with real values, the current  
 273 load and the resources left for tasks execution, respectively. Both can be  
 274 delivered by specific processes (their presentation is beyond the scope of the  
 275 current paper).  $z_t$  can be also depicted in the interval  $[0, 1]$  by dividing it into

276 equal sub-intervals. For instance, if we want to incorporate four priorities,  
 277 the first could be depicted by the value 0.25, the second by the value 0.50  
 278 and so on. In addition,  $b_t$  represents the complexity of each task related to  
 279 the required calculations to conclude the final result.  $b_t$  is ‘profiled’ in each  
 280 task and its calculation is beyond the scope of the current work. However, we  
 281 could also separate the interval  $[0, 1]$  into equal sub-intervals as in the  $z_t$  case.  
 282 For instance, if we focus on the following complexities,  $n \log n, n^2, 2^n$ , the first  
 283 could be depicted by 0.33, the second by 0.66 and the third by 1.00. In  
 284 this approach, the available complexities should be sorted in an ‘increasing’  
 285 order.

286 The discussed nodes form a graph  $G = (\mathcal{N}, E)$  where  $E$  is the set of edges  
 287 connecting the nodes. Each connecting edge  $e_{ij} \in E$  defines the communi-  
 288 cation channel between nodes  $n_i$  and  $n_j$  and is characterized by a communi-  
 289 cation cost  $\kappa_{ij} \in \mathbb{R}^+$ . At pre-defined intervals, nodes exchange information  
 290 about their status including their load and remaining resources to support  
 291 the distributed decision making process. The discussed message is in the form  
 292  $\langle l_j, r_j, \tau_j \rangle$  where the index  $j$  refers to the  $j$ th node.  $\tau_j$  is defined through the  
 293 calculation of the number of tasks successfully concluded in a time interval  
 294 (i.e., the throughput of the node). The message is processed locally to create  
 295 a tuple for each peer. Initially,  $n_i$  checks if  $T_{it}$  can be executed locally, thus,  
 296 the communication cost is  $\kappa_{ii} = 0$  and the time for starting the execution is  
 297 limited (decision D1 - Action 1). The first decision is made using the TRT  
 298 which represents the context of  $n_i$  and the requirements of the task. If the  
 299 decision is negative,  $n_i$  checks if  $T_{it}$  can be executed by its neighborhood  
 300  $\mathcal{N} \setminus \{n_i\}$ . The second decision is based on the tuples  $\langle l_j, r_j, \tau_j, \kappa_{ij} \rangle$  as derived  
 301 by the reported messages. In such case, the cost for starting the execution is  
 302 analogous to the  $\kappa_{ij}$ . It should be noted that  $\kappa_{ij}$  is dynamically adapted to  
 303 the network conditions. When nodes exchange their statuses at pre-defined  
 304 intervals, they also conclude the cost  $\kappa_{ij}$  with the ‘assistance’ of the afore-  
 305 mentioned messages maintaining the calculated historical values for future  
 306 use. The second decision is based on the distance between the task char-  
 307 acteristics and the status of each node accompanied by the communication  
 308 cost. Again, if no node could be selected for assigning  $T_{it}$ ,  $n_i$  decides to send  
 309  $T_{it}$  to Fog/Cloud with an increased communication cost; higher than the  
 310  $\max(\kappa_{ij}), \forall j$ . In Figure 2, we present the discussed internal decision process.

311 **Motivating Example.** Assume that we want to monitor a forest for  
 312 detecting emergency situations like fires. A set of nodes are placed in the  
 313 forest and are responsible to collect various data like temperature, humidity,

etc. Nodes are characterized by specific resources and can store limited amounts of data (usually, a window of the collected measurements) for performing a simple processing. The area covered by the forest, is separated into a number of sub-areas, thus, a set of nodes may observe the same sub-area. In the back end system placed at the Cloud, there is the opportunity for end users to define their queries and get information about the current status of the forest. These queries may be separated into a number of sub-queries, i.e., tasks that should be responded by the available nodes. When a query is fired, its sub-queries are reported to a node that should respond as soon as possible. For instance, the node can be instructed to report the average measurements for a time interval or to apply regression models and so on. Every node after the reception of each task checks its resources, its load as well as task's characteristics and decide if it will be executed locally. If not, the node selects the most appropriate peer (a node located in the same sub-area) to allocate the task for execution. Otherwise, the node sends the task to an application performing mathematical calculations placed in the Cloud and wait for the final response facing increased latency that will affect the final response time.

As mentioned, at pre-defined intervals, nodes exchange their load, remaining resources and speed to provide a view on their status to peer nodes. These intervals should not be low as the network will be flooded by the performance messages affecting the communication cost  $\kappa$ , however, they should not be high as nodes will not have an 'fresh' view on the performance of their peers. In any case, in the time between the intervals possible changes may happen in the performance of nodes; it consists of a stochastic process, thus, nodes cannot have a view on the completion time of each task that may vary. Furthermore, for eliminating the completion time we can increase/enhance nodes' characteristics/resources, however, this is very difficult to happen in a 'working' network. Let  $x$  is the time observed to get a response for a task. We also get  $z$  as the waiting time for a task to be executed and  $q$  as the completion time. The following equation stands true:  $x = z + q$ . Both  $z$  and  $q$  are stochastic variables affected by various parameters. For instance,  $z$  can be affected by the number of tasks waiting in the execution queue. Suppose, we are able to estimate  $q$  either a task is executed locally or in a peer or in Fog/Cloud. Then,  $x$  heavily depends on  $z$ . There are two approaches that may be adopted in our scenario. The decision for the local execution is made on top of (i)  $q$  or (ii)  $z$ . When the decision is based on  $q$ , we try to minimize the time for starting and executing future tasks, i.e., this is a

type of a priority scheme. In this scheme, the task with the lowest  $q$  has the highest priority and it will be executed first. Such an approach is typical in operating systems for the management of processes [42]. However, it is known that priority schemes suffer from starvation, i.e., indefinite blocking of tasks that exhibit high completion time. When the decision for a task execution is made based on  $z$ , we have the following choices: (i) execute it locally with  $z$  being the time for which the task will wait in the local execution queue; (ii) execute it in a peer with  $z$  being equal to the transmission time plus the time for which the task will wait in the peer's execution queue; (iii) execute it in the Fog/Cloud with  $z$  being equal to the transmission time plus the latency for starting the execution of the task and getting the final result. However, Cloud offloading almost always incurs an additional 100 to 200 ms latency compared to using edge computing solutions [7]. In this paper, our view is that tasks should be processed in a sequential order to avoid possible starvation effects and propose a model that tries to eliminate the waiting time before the execution of a task starts. An hybrid solution, i.e., a model that focuses not only on the elimination of  $z$  but, in parallel, in handling a priority scheme (based on the lowest  $q$ ) is part of our future research agenda.

The proposed decision making mechanism is a function  $g : \{TRT_t, \langle l_j, r_j, \tau_j, \kappa_{ij} \rangle\} \rightarrow \{A\}$  where  $A$  is the set of the available actions defined as follows:  $A = \{a_1, a_2, a_3, \dots\}$ . In our case,  $A = \{n_i, \{n_{selected}, \emptyset\}\}$ .  $n_i$  is the node deciding for  $T_{it}$  and  $n_{selected}$  is the peer selected to host/execute  $T_{it}$  when it is subject of a transfer. A formal definition of the available decisions is:

- **Decision 1.** Apply the current TRT in the decision making mechanism  $g$  and decide if  $T_{it}$  can be locally executed; possible actions  $\{a_1 = n_i, \{a_2 = n_{selected}\}\}$ .
- **Decision 2.** If  $T_{it}$  cannot be locally executed, decide the peer node where  $T_{it}$  will be transferred for execution; possible actions  $\{a_2 = n_{selected}, a_3 = \emptyset\}$ . If no peer is appropriate for executing  $T_{it}$ , send  $T_{it}$  to the upper layer (Fog/Cloud); action  $\{a_3 = \emptyset\}$ .

**Proposition 1.** Function  $g$  concludes the one-step optimal execution of  $T_{it}$  w.r.t. actions  $a_1, a_2, a_3$  based on  $TRT_t$  and context vectors  $\langle l_j, r_j, \tau_j, \kappa_{ij} \rangle$ .

*Proof:*  $g$  delivers the final action  $a_i$  based on a sequential processing. It applies the *principle of optimality* [36], which implies that every decision

388 should be optimal for the remaining problem (initially, we select between  
 389 three actions, next, we select between two actions). Actually,  $g$  applies the  
 390 one-step optimality process. As the time and remaining resources are the crit-  
 391 ical parameters,  $g$ , initially, examines the possibility of executing  $T_{it}$  locally  
 392 taking into consideration the parameters  $l_t, r_t, z_t, b_t$  and communication cost  
 393  $\kappa_{ii} = 0$ . The local execution of  $T_{it}$  secures that the time required for starting  
 394  $T_{it}$  is limited. In addition, the decision is made taking into consideration the  
 395 load and remaining resources. Hence, if the node has enough resources to  
 396 conclude on  $T_{it}$  will decide the local execution. On top of these parameters,  
 397 it derives the optimal result which is one of:  $\{n_i, \mathcal{N} \setminus \{n_i\}\}$ . When, the deci-  
 398 sion  $\{\mathcal{N} \setminus \{n_i\}\}$  is made,  $g$  examines the execution of  $T_{it}$  in the neighboring  
 399 nodes to (again) limit the starting time. In this case, there will be a com-  
 400 munication/transfer cost in terms of time and resources. However,  $g$  derives  
 401 the result which will be one of the following:  $\{n_{selected} \in \mathcal{N} \setminus \{n_i\}, \emptyset\}$ . The  
 402 decision is optimal in terms of time and resources as the execution of  $T_{it}$  in  
 403  $n_{selected} \in \mathcal{N} \setminus \{n_i\}$  is concluded based on the  $T_{it}$  and  $n_{selected}$  characteristics.  
 404  $g$  applies a utility maximization decision making for optimally deciding the  
 405 appropriate action. When  $\{\emptyset\}$  is the final decision,  $T_{it}$  will be transferred  
 406 to the Fog/Cloud which is, again, the optimal decision as no node in the  
 407 group can efficiently execute  $T_{it}$  based on the set of realized constraints and  
 408 task's/nodes' characteristics.  $\square$

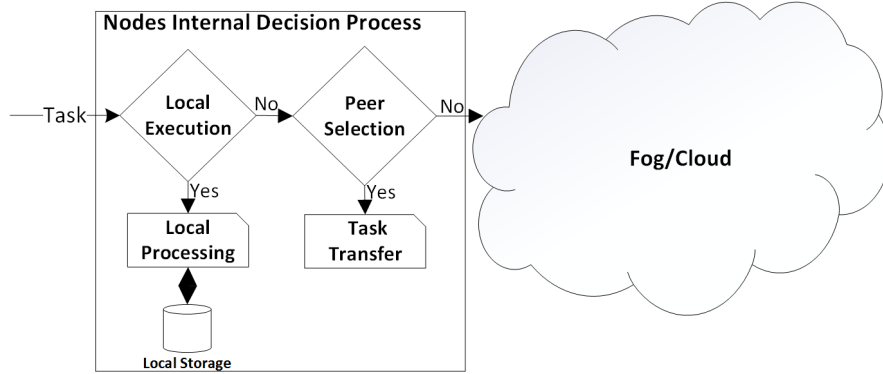


Figure 2: The internal decision process of each node. A sequential decision making is fired for each incoming task.

## 409 4. The Task Allocation Scheme

410 Every node should apply the proposed scheme in a number of tasks arriv-  
411 ing through streams. For the realization of the proposed scheme, we rely on  
412 techniques that take into consideration the combination of the available con-  
413 textual data (the aforementioned tuples) before finalizing the outcome. The  
414 adopted techniques can deliver the result in the minimum time as we aim to  
415 support (near) real-time IoT applications. For concluding on the **Decision**  
416 **1**, we rely on the  $k$ -Nearest Neighbors ( $k$ NN) classification [20], while for  
417 the **Decision 2**, we adopt the principles of utility theory [17]. Our previous  
418 work presented in [24] deals with the same problem as our current effort,  
419 however, it solves it through the adoption of a capacity model. In [24], we  
420 propose a scheme for selecting the most significant tasks to be executed at  
421 the edge providing a model for defining the significance level of a task and  
422 taking into consideration the energy constraints of nodes. Usually, capac-  
423 ity schemes suffer from the conversion process into the mathematical model.  
424 In addition, it is difficult to ‘aggregate’ multiple parameters into the same  
425 model and get the final result in a reasonable time (it depends on the num-  
426 ber of parameters). Our current effort ‘sees’ the problem as a process that  
427 classifies a task into two classes, i.e., the local execution or the transfer to  
428 another node/Fog/Cloud. In the respective literature, one can find a number  
429 of research efforts that handle a resource allocation model as a classification  
430 problem [8], [15], [31], [45], [52]. The advantage is that classification models  
431 may incorporate the relationships between the adopted parameters and can  
432 be based on past experiences as represented by historical values. In addition,  
433 the separation of the solution environment into a set of classes, it can simplify  
434 the environment reducing the confusion about the appropriate solution.

### 435 4.1. $k$ NN Classification

436 The local decision making depends on a training dataset and a  $k$ NN Clas-  
437 sifier ( $k$ NNC). We select such a technique, as  $k$ NNCs exhibit ease interpre-  
438 tation, low calculation time and acceptable predictive power when compared  
439 with other techniques, e.g., logistic regression, random forests. In addition, a  
440  $k$ NNC is non parametric, which means that it makes no explicit assumptions  
441 about the form of the function producing the final result. However, it heavily  
442 depends on the provided training dataset. The  $k$ NNC decides whether the  
443 node receiving  $T_{it}$  can/should execute it locally or not. This decision is made  
444 based on the  $TRT_t$  i.e.,  $\langle l_t, r_t, z_t, b_t \rangle$ .

445 The  $k$ NNC is based on learning by analogy, i.e., it compares the given  
 446 tuple with the training tuples to identify the similar ones. The training  
 447 tuples and the incoming tuples are characterized by the same number of  
 448 variables/attributes. The training tuples can be extracted by a statistical  
 449 analysis process performed on top of historical values. Such historical values  
 450 are recorded (e.g., for a warm up period) and adopted to build the classifier.  
 451 It becomes obvious that, in this process, the intervention of experts that will  
 452 define the final class for each tuple is required. The  $k$ NNC searches in the  
 453 dimensional space (let  $Y$  be the number of variables/dimensions), the pattern  
 454 space that is close to the incoming tuple. We consider that closeness is  
 455 defined through the adoption of the Euclidean distance, i.e.,  $d(\mathbf{TRT}_t, \mathbf{TRT}_s)$ ,  
 456  $\forall s$ ;  $s$  is the index of each training tuple met in the available dataset  $D$ .  
 457 Actually,  $D$  consists of multiple  $TRT$ s accompanied by the appropriate action  
 458 for each one (local execution or not). Other distance measures could be also  
 459 adopted e.g., Manhattan, Minkowski, Hamming. Let  $y_i$  be the  $i$ th variable  
 460 in the  $TRT$ s (i.e.,  $y_i \in \{l, r, z, b\}$ ). Then, the aforementioned Euclidean  
 461 distance is defined as:  $d(\mathbf{TRT}_t, \mathbf{TRT}_s) = \sqrt{\sum_{i=1}^{|D|} (y_{i,TRT_t} - y_{i,TRT_s})^2}$ . The  
 462 closeness between the incoming tuple and the training tuples is based on the  
 463 difference of the numeric values for each variable. The  $k$ NNC estimates the  
 464 conditional probability for each class. There are two classes in our case; the  
 465 local execution depicted by the action  $a_1 = \{n_i\}$  and the transfer to peers  
 466 depicted by the action  $a_2 = \{\mathcal{N} \setminus \{n_i\}\}$ . The probability is translated as the  
 467 fraction of points with the corresponding class label. The incoming tuple is  
 468 assigned to the most common class among the  $k$  nearest neighbors i.e., the  
 469 class with the highest probability. The value for  $k$  is selected to be the value  
 470 that minimizes the error rate and it is derived through simulations.

#### 471 4.2. Peer Selection Scheme

472 The second decision of our scheme is related with the identification and  
 473 the selection of the appropriate node for allocating any ‘rejected’ task. For  
 474 this decision, we rely on the principles of the Utility Theory [17]. We focus  
 475 on the multi-attribute utility theory [23] where we consider that each peer  
 476 is characterized by the above discussed tuples  $\langle l_j, r_j, \tau_j, \kappa_{ij} \rangle$ . In this section,  
 477 the notion of ‘attribute’ is the same with the notion of variable/dimension  
 478 adopted in the previous sections. As every node is characterized by multiple  
 479 attributes, we aim to ‘combine’ them and provide a final ranking to select  
 480 the most appropriate peer. Multi-attribute utility theory concerns with ex-  
 481 pressing the utilities of multiple attributes (called as individual utilities) as a



function of the utilities of each attribute taken singly [17]. Our approach focuses on the selection of the most desirable alternatives among many different alternatives. In theory, many functions can be adopted for the calculation of individual utilities. For instance, we could rely on additive, multiplicative or multi-linear functions. However, as studied in [23], for four or more attributes, the reasonable models are the additive and the multiplicative schemes. In our case, we adopt both of them and provide two rankings of the available peers. Afterwards, we aggregate the two ranked lists and select the node present in the first place of the final aggregated list. If no node in the final list exhibits an aggregated result above a pre-defined threshold, the task will be allocated for execution in the Fog/Cloud. The above described process is fired for every  $T_{it}$  for which the action  $a_2$  is decided.

As mentioned, in  $n_i$ , there is available information for the status of peers, i.e.,  $\langle l, r, \tau, \kappa \rangle$ . Our model can be easily extended to involve more attributes. For some attributes, we desire to enjoy a low value close to 0 to gain high utility (e.g.,  $l, \kappa$ ) while for others, we aim at high values close to unity to gain high utility (e.g.,  $r, \tau$ ). The former attributes are called *non-proportional*, while the latter are called *proportional*. For each attribute  $y_s$ ,  $s = 1, 2, \dots, Y$ , we define the individual utility function  $f(y_s)$  based on the exponential distribution. For proportional attributes, we get  $f(y_s) = e^{-\gamma y_s + \delta}$  while for non-proportional attributes we get  $f(y_s) = \frac{1}{e^{-\gamma y_s + \delta}}$ . Parameters  $\gamma$  and  $\delta$  are adopted to produce values in the interval  $[0, 1]$  and affect the final utility. For instance, we can follow more ‘strict’ strategies where the utility abruptly falls to zero when an attribute exceeds a threshold or be more relaxed concerning that the tendency is smoother than in the previous example.

These single/individual utility functions are initially ‘combined’ with the additive function:  $U_{ADD}(y_1, y_2, \dots, y_Y) = \sum_{s=1}^Y w_s f(y_s)$ , with  $\sum_{s=1}^Y w_s = 1.0$ . In the case of the multiplicative function, the following equation stands true:  $U_{MUL}(y_1, y_2, \dots, y_Y) = \prod_{s=1}^Y w_s f(y_s)$ . In general, the definition of the appropriate weights is a strategic decision based on the attributes we want to pay increased attention when we calculate the weighted result. In the relevant literature, one can find various efforts that propose automated ways to calculate the most appropriate weights. Some of these models are the Min-Max principle [18], optimization approaches [43] or geometric programming [21], [44]. The adoption of an intelligent technique can facilitate the dynamic definition of weights according to the characteristics of the environment. However, this dynamic approach is beyond the scope of the current work. Based on  $U_{ADD}$  and  $U_{MUL}$ , we provide two ranked lists of the peers

in a descending order. Peers in the first place of the lists offer the highest possible utility when  $T_{it}$  will be allocated to them.

The final step is the aggregation of the two lists, i.e.,  $\mathbf{U}_{ADD}$  and  $\mathbf{U}_{MUL}$ . For the provision of the final list  $\mathbf{U}$ , we rely on a simple and fast technique, i.e., the Borda count model [13]. We consider that the aforementioned lists are preferences of peers retrieved by the corresponding functions. The peer present in the first place of a list gets  $|\mathcal{N}| - 1$  points, the second gets  $|\mathcal{N}| - 2$  points and so on. The final list  $\mathbf{U}$  is created through the averaging of the points collected by the two lists.  $\mathbf{U}$  is, finally, sorted in descending order. If no node exhibits a result over a pre-defined threshold, the task is allocated to the Fog/Cloud otherwise, the first node will host  $T_{it}$ . The pre-defined threshold could be delivered through simulations or through a dynamic threshold optimization model to derive the most appropriate value for each instance of the problem [11], [14], [50].

## 5. Estimating the Load of Nodes

### 5.1. The Short Term Expected Load

As nodes process a number of tasks, their load will be affected by their report rate. The more the number of tasks, the higher the load becomes. Recall that the load of nodes affect the decisions related to the location of the execution of each task. In this section, we provide an analysis on the short term expected load for each node to have a view on the parameters that affect their performance. The short term expected load is related to the number of tasks that will be executed locally after their initial allocation. We consider that multiple ‘execution eras’ deal with the execution of tasks reported in  $G$ . At every era, nodes receive a number of tasks and apply the proposed sequential decision making process. Let us define the following events: **(i)** M1:  $T_{it}$  arrives at  $n_i$ ; **(ii)** M2:  $n_i$  decides the action  $a_1$ . Without loss of generality, we consider that these events are independent. The decision for action  $a_1$  (i.e., event M2 - the local execution of  $T_{it}$ ) depends on the expected number of the incoming tasks at  $n_i$  and the probability of local execution. The arrival of tasks in  $G$  can be modeled as a Poisson process with rate  $\lambda$  while the decision for local execution can be seen as a Bernoulli trial with probability of success  $p = P(M2)$ . A Poisson process arises when there is a large number of sources that produce events independently, e.g., arrivals, requests to a server, etc [32]. In addition, a trial (e.g., a local decision making)

where only two outcomes are possible (e.g., local execution of a task or not) can be modeled as a Bernoulli trial [49].

**Proposition 2.** The expected number of tasks arriving at  $n_i$  is  $\frac{\lambda}{|\mathcal{N}|}$ .

*Proof:* We consider that  $|T|$  tasks arrive in  $G$  with a rate  $\lambda$  in a time unit (e.g., an hour, a day, a week). The arrival of tasks in  $G$  follows a Poisson distribution while the initial ‘allocation’ of tasks follows a Uniform distribution, i.e., reporting every  $T_{it}$  to  $n_i$ . Based on the Poisson distribution, the expected number of tasks reported to  $n_i$  is:  $\lambda \frac{1}{|\mathcal{N}|} = \frac{\lambda}{|\mathcal{N}|}$ .  $\square$

$n_i$  after the reception of  $T_{it}$  checks the available training dataset and applies the  $k$ NNC. The probability of the local execution, then, depends on the ‘class’ indicated by the majority of the  $k$  neighbors. Any decision for local execution indicates that the majority of the  $k$ NNs report the action  $a_1$ , thus, the ‘class’  $n_i$ . Initially, we assume that values for each variable/dimension  $y$  follows the Gaussian distribution. In general, a continuous-valued variable is typically assumed to have a Gaussian distribution to easily estimate the distribution’s parameters (i.e., mean and standard deviation) from training samples [20].

**Lemma 1.** The probability of locally executing  $T_{it}$  when the Gaussian distribution is assumed is

$$p = \sum_{m=\lfloor \frac{k}{2}+1 \rfloor}^k \binom{k}{m} \left( \frac{\pi_1}{|\mathcal{N}|\pi_2} \right)^m \left( 1 - \frac{\pi_1}{|\mathcal{N}|\pi_2} \right)^{k-m}$$

$$\text{where } \pi_1 = \prod_{\forall s} \frac{1}{\sigma_{n_i}} e^{-\frac{(y_s - \mu_{n_i})^2}{2\sigma_{n_i}^2}} \text{ and } \pi_2 = \prod_{\forall s} \frac{1}{\sigma_s} e^{-\frac{(y_s - \mu_s)^2}{2\sigma_s^2}}.$$

*Proof:* For calculating  $p$ , we should calculate the probability of having the majority of the  $k$  neighbors indicating the class  $n_i$ . The probability of the majority among the  $k$  neighbors is [26]:  $P(\text{majority}) = \sum_{m=\lfloor \frac{k}{2}+1 \rfloor}^k \binom{k}{m} (p')^m (1-p')^{k-m}$  where  $p'$  is the probability of having the  $m$ th neighbor at the correct class (i.e., the tuple indicating local execution - class  $n_i$ . Under the assumption that variables/dimensions follow the Gaussian distribution, the probability of having the  $TRT_t$  ‘generated’ by the  $n_i$  is  $P(n_i|TRT_t)$ . Based on the Bayes theorem, we get:  $P(n_i|TRT_t) = \frac{P(TRT_t|n_i)P(n_i)}{P(TRT_t)}$ . However,  $P(n_i) = \frac{1}{|\mathcal{N}|}$ . In addition,  $P(TRT_t) = \prod_{\forall s} \left( \frac{1}{\sqrt{2\pi}\sigma_s} e^{-\frac{(y_s - \mu_s)^2}{2\sigma_s^2}} \right)$  where  $\mu_s$  and  $\sigma_s$  are the mean and the deviation of the  $s$ th variable/dimension as calculated through the training dataset. In addition,  $y_s$  is the  $s$ th variable in the  $TRT$ s (i.e.,  $y_s \in \{l, r, z, b\}$ ). Finally, we get  $P(TRT_t|n_i) = \prod_{\forall s} \left( \frac{1}{\sqrt{2\pi}\sigma_{n_i}} e^{-\frac{(y_s - \mu_{n_i})^2}{2\sigma_{n_i}^2}} \right)$  where  $\mu_{n_i}$  and  $\sigma_{n_i}$  are the mean and the deviation of the  $s$ th variable/dimension for tuples classified in the local execution class. Through calculations, we get the final equation

590 as presented by the Lemma.  $\square$

591 Based on the probability indicated by the Lemma 1, we can easily cal-  
 592 culate the short term expected load  $E(l)$  for each node just after the initial  
 593 allocation of the incoming tasks.  $E(l)$  can be extracted by the Binomial dis-  
 594 tribution corresponding to the aforementioned Bernoulli trial when having  
 595  $|Q|$  tasks for local execution.

596 **Lemma 2.** The short term expected load for each node in the network  
 597 when the Gaussian distribution is assumed is

$$598 \quad E(l) = \frac{\lambda}{|\mathcal{N}|} \left(1 - \frac{\pi_1}{|\mathcal{N}|\pi_2}\right)^k \sum_{m=\lfloor \frac{k}{2}+1 \rfloor}^k \binom{k}{m} \left(\frac{\pi_1}{|\mathcal{N}|\pi_2-\pi_1}\right)^m \text{ where } \pi_1 = \prod_{\forall s} \frac{1}{\sigma_{n_i}} e^{-\frac{(y_s-\mu_{n_i})^2}{2\sigma_{n_i}^2}}$$

599 and  $\pi_2 = \prod_{\forall s} \frac{1}{\sigma_s} e^{-\frac{(y_s-\mu_s)^2}{2\sigma_s^2}}$ .

600 *Proof:* The short term expected load of a node is the sum of the expected  
 601 number of tasks multiplied with the probability of locally executing a task.  
 602 From the Proposition 1, we have that the expected number of tasks that will  
 603 be reported to  $n_i$  is  $\frac{\lambda}{|\mathcal{N}|}$ . For any Binomial distribution, the expected value  
 604 is derived by:  $\sum_{i=1}^{|Q|} i \binom{|Q|}{i} p^i (1-p)^{|Q|-i}$ , where  $|Q|$  is the number of the tasks  
 605 reported locally. Based on the Binomial theorem, we can easily conclude  
 606 that the expected value of the Binomial is  $|Q|p$  (we omit the proof as it is  
 607 widely studied). Based on the Lemma 1 and through substitutions, we can  
 608 easily derive  $E(l)$  as depicted by the Lemma 2.  $\square$

609 For providing a complete analysis of the problem, we also focus on the  
 610 adoption of the Uniform distribution to depict the value of each attribute.

611 **Lemma 3.** The probability of locally executing  $T_{it}$  when the Uniform  
 612 distribution is adopted is  $p = \left(\frac{|\mathcal{N}|-1}{|\mathcal{N}|}\right)^k \sum_{m=\lfloor \frac{k}{2}+1 \rfloor}^k \binom{k}{m} \frac{1}{(|\mathcal{N}|-1)^m}$

613 *Proof:* For calculating  $p$ , we follow the same approach as in Lemma 1.  
 614 However, the probability density function is constant in the Uniform distri-  
 615 bution case. Through the same calculations as in Lemma 1, we get the final  
 616 equation as presented by the current Lemma.  $\square$

617 Based on the probability indicated by Lemma 3, we can easily calculate  
 618 the short term expected load  $E(l)$  when the Uniform distribution is adopted.

619 **Lemma 4.** The short term expected load for each node in the network  
 620 when the Uniform distribution is adopted is  $E(l) = \frac{\lambda(|\mathcal{N}|-1)^k}{|\mathcal{N}|^{k+1}} \sum_{m=\lfloor \frac{k}{2}+1 \rfloor}^k \binom{k}{m} \frac{1}{(|\mathcal{N}|-1)^m}$ .

621 *Proof:* For proving the Lemma, we adopt the same approach as in Lemma  
 622 2, however, the probability of local execution is delivered by Lemma 3. Hence,  
 623 through substitutions, we can easily derive  $E(l)$  as depicted by Lemma 4.  $\square$

## 624 5.2. The Long Term Expected Load

625 The long term expected load for each node is concluded through the  
626 transfer of tasks in the network. It consists of the load in an ‘execution  
627 era’ after multiple tasks rejections and transfers. In our model, we consider  
628 that after  $\Omega$  decisions/transfers, every node assigns the ‘rejected’ tasks to the  
629 Fog/Cloud.  $\Omega$  is a parameter with a strategic meaning; a high value will lead  
630 the ‘rejected’ tasks to ‘circulate’ among nodes till their final execution. In this  
631 case, tasks are transferred between nodes till they ‘find’ a node that will un-  
632 dertake the responsibility of their execution. This could happen when nodes  
633 characteristics indicate that the load and the resources (are dynamically up-  
634 dated) can support the action  $a_1$ . When  $\Omega \rightarrow \infty$ , the proposed model forces  
635 the tasks to be circulated to the network till a node decides their execution,  
636 thus, the ‘execution era’ is implicitly extended. However, in that case, the  
637 time required for the transfers and the communication overhead should be  
638 compared with the delay/latency realized when tasks’ execution is concluded  
639 in the Fog/Cloud. In our model,  $\Omega$  is defined based on the average latency  
640 for executing tasks in the Fog/Cloud and considering a minimum time for  
641 realizing a task transfer from a node to another. For instance, simulations in  
642 [27] show that the average latency for executing tasks in the Cloud is over  
643 24 milliseconds when the tasks arrival rate increases. A low  $\Omega$  indicates a  
644 limited number of ‘hops’ till tasks’ transfer to the Fog/Cloud. Our future  
645 research plans is to define an intelligent model for delivering the final  $\Omega$ .

646 Recall that with probability  $p$ , each node decides to locally execute a task,  
647 thus, with probability  $1 - p$  a task is ‘rejected’. After receiving  $\frac{\lambda}{|\mathcal{N}|}$  tasks,  
648  $n_i$  will accept (i.e., locally execute)  $\frac{\lambda}{|\mathcal{N}|}p$  tasks and will transfer  $\frac{\lambda}{|\mathcal{N}|}(1 - p)$   
649 tasks to the network. In the ‘worst’ case, after the first decision, all the  
650 ‘rejected’ tasks could be transferred to the same peer; the same could be  
651 true for the remaining nodes. In this case, a single node, e.g.,  $n_{selected}$ , in  
652 the entire network, will host  $\frac{\lambda}{|\mathcal{N}|} \sum_{\forall i, i \neq j} (1 - p_i)$  while the long term expected  
653 load of the remaining nodes will be limited.

654 Without loss of generality, let us focus on the ‘average’ case. In the  
655 average case,  $n_i$ , after every decision, uniformly distributes the ‘rejected’  
656 tasks to the available  $|\mathcal{N}| - 1$  peers. This means that  $n_i$  will distribute  
657  $\frac{\lambda}{|\mathcal{N}|(|\mathcal{N}|-1)}(1 - p_i)$  tasks to each of its peers. However, when  $n_i$  distributes the  
658 ‘rejected’ tasks, at the same time, the remaining nodes send their ‘rejected’  
659 tasks into the network as well. Hence, each node *distributes* and *receives* a  
660 number of tasks that are ‘rejected’ after every decision made at the round

661  $\omega \in \{1, 2, 3, \dots, \Omega\}$ . It should be noted that during the distribution of tasks,  
 662 nodes continue to execute the ‘accepted’ tasks, thus, their characteristics are  
 663 updated (e.g., their load).

664 **Lemma 5.** The long term expected load for each node, at the  $\omega$  decision  
 665 round, is a function of the success probabilities  $p_i, i = 1, 2, \dots, |\mathcal{N}|$  calculated  
 666 for every node in the network based on their characteristics.

667 *Proof:* In Table 1, we present the load for two decision rounds. In general,  
 668  $n_i$  at  $\omega$  will receive  $\frac{\lambda}{|\mathcal{N}|(|\mathcal{N}|-1)^{\omega-1}} \left( \sum_{j=1, j \neq i}^{|\mathcal{N}|} (1 - p_j) \right)^{\omega-1}, \omega \in \{1, 2, \dots, \Omega\}$ .  
 669 From those tasks, the number of the locally executed will be  
 670  $\frac{\lambda}{|\mathcal{N}|(|\mathcal{N}|-1)^{\omega-1}} \left( \sum_{j=1, j \neq i}^{|\mathcal{N}|} (1 - p_j) \right)^{\omega-1} p_i$  which is a function of the success  
 671 probabilities calculated for each node in the network.

Table 1: Incoming and Outgoing Tasks for three decision steps.

$\omega$	Tasks		
	Incoming	Locally Executed	Outgoing
1	$\frac{\lambda}{ \mathcal{N} }$	$\frac{\lambda}{ \mathcal{N} } p_i$	$\frac{\lambda}{ \mathcal{N} } (1 - p_i)$
2	$\frac{\lambda}{ \mathcal{N} ( \mathcal{N} -1)} \sum_{j=1, j \neq i}^{ \mathcal{N} } (1 - p_j)$	$\frac{\lambda}{ \mathcal{N} ( \mathcal{N} -1)} \sum_{j=1, j \neq i}^{ \mathcal{N} } (1 - p_j) p_i$	$\frac{\lambda}{ \mathcal{N} ( \mathcal{N} -1)} \sum_{j=1, j \neq i}^{ \mathcal{N} } (1 - p_j)(1 - p_i)$

672 □  
 673 Based on Lemmas 2 and 5, we can easily calculate the final long term  
 674 expected load for each node for an ‘execution era’. We consider that the  
 675 next era will start only after the final execution for every incoming task (i.e.,  
 676  $\Omega \rightarrow \infty$ ).

677 **Lemma 6.** The long term expected load for a node  $n_i$  is  $E(l) =$   
 678  $\frac{\lambda(|\mathcal{N}|-1)}{|\mathcal{N}|(|\mathcal{N}|-1-\chi)} \cdot p_i$  where  $\chi = \sum_{j=1, j \neq i}^{|\mathcal{N}|} (1 - p_j)$ .

679 *Proof:* The long term expected load will be calculated based on the  
 680 Lemma 5 for the entire set of values of  $\omega$ . We consider that  $\Omega \rightarrow \infty$ .  
 681 Hence, we should calculate the sum of the number of tasks multiplied by  
 682 the probability of success for  $\omega = 1, 2, \dots, \Omega$ . Based on the Lemma 5,  
 683 we get that the expected number of tasks that will be locally executed is:  
 684  $\frac{\lambda}{|\mathcal{N}|} p_i + \frac{\lambda}{|\mathcal{N}|(|\mathcal{N}|-1)} \left( \sum_{j=1, j \neq i}^{|\mathcal{N}|} (1 - p_j) \right) p_i + \frac{\lambda}{|\mathcal{N}|(|\mathcal{N}|-1)^2} \left( \sum_{j=1, j \neq i}^{|\mathcal{N}|} (1 - p_j) \right)^2 p_i +$   
 685  $\dots = \frac{\lambda}{|\mathcal{N}|} p_i \sum_{\omega=1}^{\Omega} \frac{\chi^{\omega-1}}{(|\mathcal{N}|-1)^{\omega-1}},$  with  $\chi = \sum_{j=1, j \neq i}^{|\mathcal{N}|} (1 - p_j)$ . We observe that  
 686  $\frac{\chi}{(|\mathcal{N}|-1)} < 1$ , thus, the final long term expected load is the result of the sum  
 687 of an infinite geometric series, i.e.,  $E(l) = \frac{\lambda(|\mathcal{N}|-1)}{|\mathcal{N}|(|\mathcal{N}|-1-\chi)} \cdot p_i.$  □

688 An interesting observation is that if  $p_i$ s for the  $|\mathcal{N} - 1|$  peers are equal to  
 689 zero, the expected load of  $n_i$  will be infinite. This scenario depicts the above  
 690 discussed worst case scenario.

## 691 6. Experimental Evaluation

692 In our experimental evaluation, we investigate whether the model is ca-  
 693 pable of *optimally deciding the local execution of each task or transferring*  
 694 *this responsibility to the appropriate peer.*

### 695 6.1. Experimental Setup & Performance Metrics

696 In our simulations, we adopt the parameters  $\langle l, r, z, b \rangle$  for decisions related  
 697 to the local execution of the incoming tasks and  $\langle l, r, \tau, \kappa \rangle$  for selecting the  
 698 appropriate peers in the network. We focus on two aspects: **(a)** The correct  
 699 identification of tasks that will be executed locally, and **(b)** The correct  
 700 identification of the appropriate peer to execute the task. For the first aspect,  
 701 we adopt the widely known metrics *precision*  $\epsilon$  and *recall*  $\zeta$ . We also adopt  
 702 the *F-measure*  $\phi$  and the *accuracy*  $\psi$  metrics. These metrics are defined as:  
 703  $\epsilon = \frac{TP}{TP+FP}$ ,  $\zeta = \frac{TP}{TP+FN}$ ,  $\phi = 2\frac{\epsilon\zeta}{\epsilon+\zeta}$ ,  $\psi = \frac{TP+TN}{TP+TN+FP+FN}$  where  $T$  refers to  
 704 'true',  $P$  refers to 'positive',  $F$  refers to 'false', and  $N$  refers to 'negative'.  
 705 Hence,  $TP$  refers to true positive events, i.e., identified events that had to be  
 706 identified,  $FP$  refers to false positive events, i.e., identified events that had  
 707 to not been identified, and so on.

708 We also evaluate the selection of the appropriate peer when a task should  
 709 be transferred to the group/neighborhood. We adopt random values for each  
 710 parameter (i.e.,  $\langle l, r, \tau, \kappa \rangle$ ). With probability 0.20, a new message arrives  
 711 to nodes indicating updates on the status of the remaining peers (i.e., load,  
 712 speed, communication cost). For evaluating the selection of the appropriate  
 713 peer, we focus on the mean of each parameter (i.e.,  $\langle l, r, \tau, \kappa \rangle$ ) over the se-  
 714 lected peers. For  $l$  and  $\kappa$ , we target on a low mean while for the remaining  
 715 parameters, we expect to observe high values. The mean is represented by  
 716 the indication  $A$  in every metric i.e.,  $\langle l_A, r_A, \tau_A, \kappa_A \rangle$ . In addition, we define  
 717 metrics for identifying if the selected peers are the best among the avail-  
 718 able nodes (optimality of the model). For this, we adopt the indication  $B$   
 719 in each metric, i.e.,  $\langle l_B, r_B, \tau_B, \kappa_B \rangle$ . The indication  $B$  in the aforementioned  
 720 parameters is used to depict the difference of the value achieved by our model  
 721 compared to the optimal value observed in peers' characteristics. We calcu-  
 722 late the optimal value (the highest or the lowest depending on the parameter)

723 between all the nodes in the network and compare it with the characteristics  
724 of the selected node. It should be noted that a node exhibiting e.g., the  
725 lowest load, it does not mean that the same node exhibits e.g., the lowest  
726 communication cost. As our model aims to get decisions based on multiple  
727 attributes, our evaluation process manages the entire set of parameters at the  
728 same time. Any negative result means that the selected node, by our model,  
729 exhibits better characteristics than the peer with the lowest load. Based on  
730 these metrics, we aim to reveal if the proposed model is capable of selecting  
731 the best possible peer to host the ‘rejected’ tasks.

732 We adopt a simulator created in Java and train the proposed decision  
733 making mechanism adopting synthetic and real data. The real dataset is  
734 adopted from [4] and concerns data related to fire detection and the calcu-  
735 lation of the affected area. From these data, we adopt the temperature, the  
736 humidity, the wind and the rain indication for feeding values to our param-  
737 eters. We assume that the indication of fire and the presence of an affected  
738 area corresponds to action  $a_1$ , i.e., the local execution of a task. Usually, the  
739 indication of a fire is characterized by a low humidity, a high temperature  
740 and a high wind <sup>1</sup>. In our scenario, the decision for the local execution of  
741 a task is supported by a high priority, a low load and a high availability  
742 of resources (the complexity is combined with the remaining parameters for  
743 the final decision making). Hence, adopting the real dataset and adapting  
744 it into our scenario, we select the rain indication to ‘virtually’ correspond  
745 to  $z$  (we consider three priorities), the humidity to  $l$  (we target to a low  
746 load to locally execute a task like a low humidity may support the indica-  
747 tion of a fire), the temperature to  $r$  (we target to high resources availability  
748 like a high temperature may support the indication of a fire) and the wind  
749 to  $b$ . Each tuple in the training dataset (either the synthetic or the real)  
750 is related to  $\langle l, r, z, b \rangle$ . The training dataset, provides various combinations  
751 of the aforementioned parameters accompanied by the appropriate decision  
752 (i.e., the corresponding action). When the tuple is classified as 1, it means  
753 that the corresponding task should be executed locally (action  $a_1$ ) while a  
754 classification value 0 indicates the decision of transferring the task to the  
755 group or Fog/Cloud (actions  $a_2$  and  $a_3$ ). In the real dataset, we add the  
756 class 1 when the temperature, the humidity, the wind and the rain indicate  
757 a fire; otherwise, we add the class 0. We also present experimental results

---

<sup>1</sup><http://learningcenter.firewise.org/Firefighter-Safety/1-6.php>



758 for the performance of our model concerning the expected load of each node.  
759 We perform the evaluation of our scheme for  $|\mathcal{N}| = \{10, 50, 100, 1000\}$ . We  
760 study how  $|\mathcal{N}|$  affects the results. In addition, we consider four (4) experi-  
761 mental scenarios: (i) Scenario A:  $\{w_s\} = \{0.3, 0.3, 0.3, 0.1\}$ ; (ii) Scenario B:  
762  $\{w_s\} = \{0.6, 0.2, 0.1, 0.1\}$ ; (iii) Scenario C:  $\{w_s\} = \{0.2, 0.2, 0.4, 0.4\}$ ; (iv)  
763 Scenario D:  $\{w_s\} = \{0.2, 0.1, 0.1, 0.6\}$ . Through the aforementioned sce-  
764 narios, we pay attention on different parameters when selecting a node for  
765 transferring the task. For instance, Scenario A pays equal attention on the  
766 load, the resources and the speed while Scenario B pays more attention on  
767 the load. Scenario C pays more attention on the speed and the cost and,  
768 finally, Scenario D pays attention on the cost.

## 769 6.2. Performance Evaluation

770 Initially, we report on the complexity of the proposed model. This com-  
771 plexity is affected by: (i) the complexity of the  $k$ NNC; (ii) the complexity  
772 of the utilities calculation; (iii) the complexity of the utilities aggregation;  
773 (iv) the complexity of the sorting process to produce the final utilities list.  
774 In the worst case, the complexity for (i) is  $O(k|D| + |D|Y)$ , where  $D$  is the  
775 training dataset,  $k$  is the number of neighbors and  $Y$  is the number of dimen-  
776 sions/variables. In Fig. 3, we present the plot of the discussed complexity. In  
777 addition, the complexity for (ii) and (iii) is  $O(|\mathcal{N}|)$  while the complexity for  
778 (iv) is  $O(|\mathcal{N}|\log|\mathcal{N}|)$  (we can rely on a fast sorting technique e.g., merge or  
779 heap sort). In Fig. 4, we keep  $Y$  constant and present the complexity of the  
780 proposed scheme for various numbers of the length of the training dataset  
781 and the number of the peers. Based on the above, the final complexity in the  
782 worst case scenario is  $O(k|D| + |D|Y + |\mathcal{N}|\log|\mathcal{N}|)$ . We compare the com-  
783 plexity of our model with other relevant efforts in the domain. In [53], the  
784 authors discuss three task scheduling algorithms, the EASU (Energy-Aware  
785 Scheduling under Uncertainty), the RAS (Reliability-Aware Scheduling) and  
786 the basic resource provisioning algorithm. The complexity of the EASU is  
787  $O(|T||VMs||\mathcal{N}|)$  where  $|VMs|$  is the number of the VMs where the tasks  
788 should be allocated and  $|\mathcal{N}|$  is the number of hosts like in our case. The  
789 complexity of the RAS is  $O(|VMs||\mathcal{N}||\mathcal{N}|_C)$  with  $|\mathcal{N}|_C$  depicting the num-  
790 ber of candidate hosts. In [35], the tasks allocation problem is seen as a  
791 capacity problem. The network is modeled as a graph like in our case. The  
792 complexity of the proposed algorithm is  $O(|\mathcal{N}| + (|\mathcal{N}|^2|T|) + |\mathcal{N}||E|^2)$  (for  
793 the calculation of the last part of the complexity we consider the Edmonds-  
794 Karp algorithm for finding the maximum flow in a graph). Finally, in [56],

the authors solve the task allocation problem through the adoption of the network flow method and conclude that the intranode communication cost is a key to the complexity of the algorithm. They prove that complexity is  $O(|\mathcal{N}|^2|T|^4)$  if the intranode communication cost equals the internode communication cost. In addition, the convex cost flow version of the algorithm can be solved in  $O(|\mathcal{N}|^2|T|^2\log(|\mathcal{N}| + |T|))$ .

In the following experiments, we try to reveal the short term expected load for each node when we adopt various realizations for parameters  $\lambda$ ,  $|\mathcal{N}|$  and  $Y$ . Our aim is to see how many tasks will be hosted locally when  $\omega = 1$ . For this, we simulate the arrival of 1,000 *TRTs* and for each one, we adopt the Uniform and the Gaussian distributions to get values for every parameter participating in the envisioned tuples. The Uniform distribution is adopted to simulate a very dynamic environment where parameters can change values allocated in the entire interval  $[0, 1]$ . On the other hand, the Gaussian distribution is adopted to simulate a more ‘stable’ environment where parameters realizations are allocated around the mean. In Figure 5, we present our results for the expected load  $E(l)$  and for different  $\lambda$ . As natural, we observe that an increment in the number of the incoming tasks in the entire network will increase the short term expected load of nodes. The interesting is that the Uniform distribution results more tasks for local execution compared to the Gaussian distribution. The reason is that the local datasets, in the Uniform distribution case, contain data that are not concentrated around the mean increasing the probability for local execution. Recall that the probability for having a task locally executed depends on the ‘similarity’ between the characteristics of every task and the available dataset adopted for delivering the  $k$ NNs, thus, the final decision. Another interesting observation is as follows. In this set of experiments, we get  $|\mathcal{N}| = 5$  while  $E(l) = \{46, 33\}$  for the Uniform and the Gaussian distributions, respectively. If we consider that 1,000 tasks arrive in the network in a time unit, thus, approximately, 200 tasks are reported at each node, only 230 and 165 tasks, respectively, will be executed locally after the first decision while the remaining will be transferred to peers or the Fog/Cloud. It should be noted that those numbers do not include the tasks that are transferred in the current node by peers.

In Figure 6, we show our results for short term  $E(l)$  and for different  $|\mathcal{N}|$ . In these plots, we do not present the results for  $|\mathcal{N}| = 1$  because it is the only result above unity. For all the remaining experimental scenarios, we get the short term  $E(l)$  below unity, which indicates that the load for each node

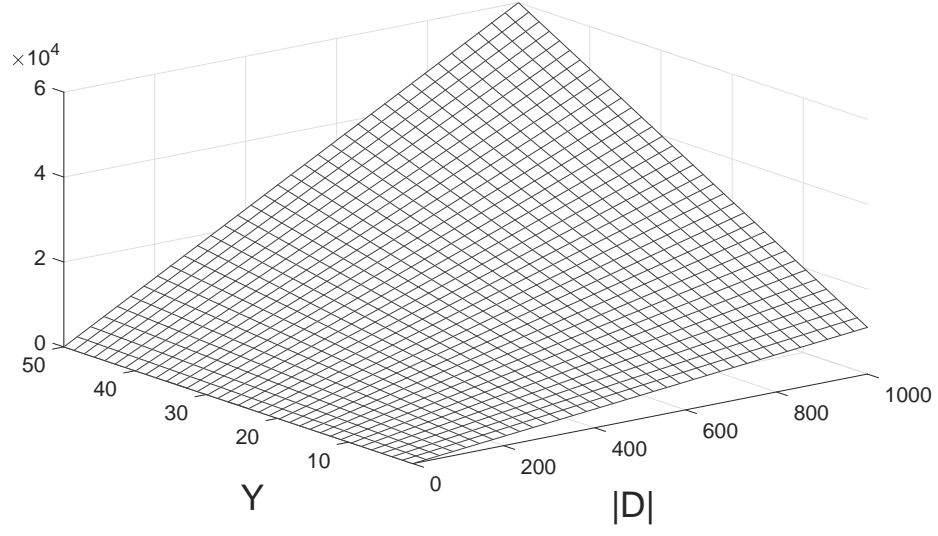


Figure 3: The complexity of the  $k$ NNC classifier.

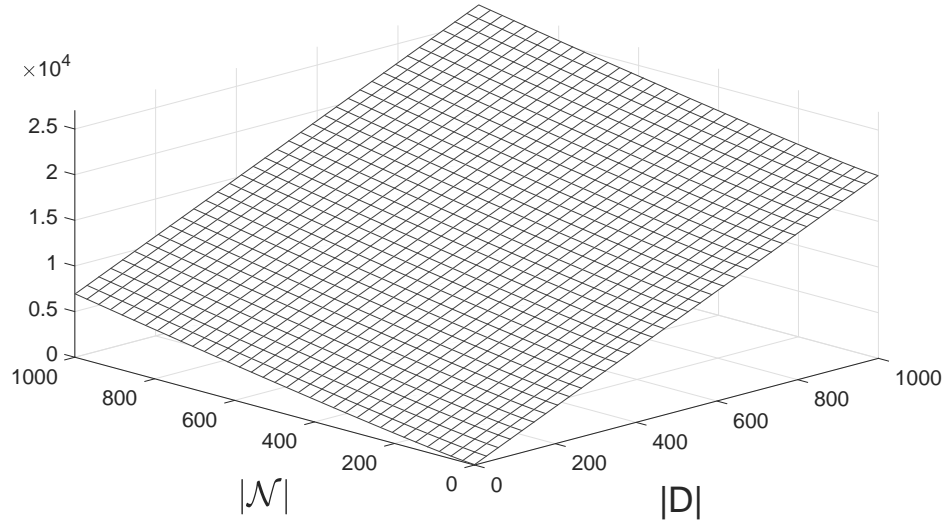
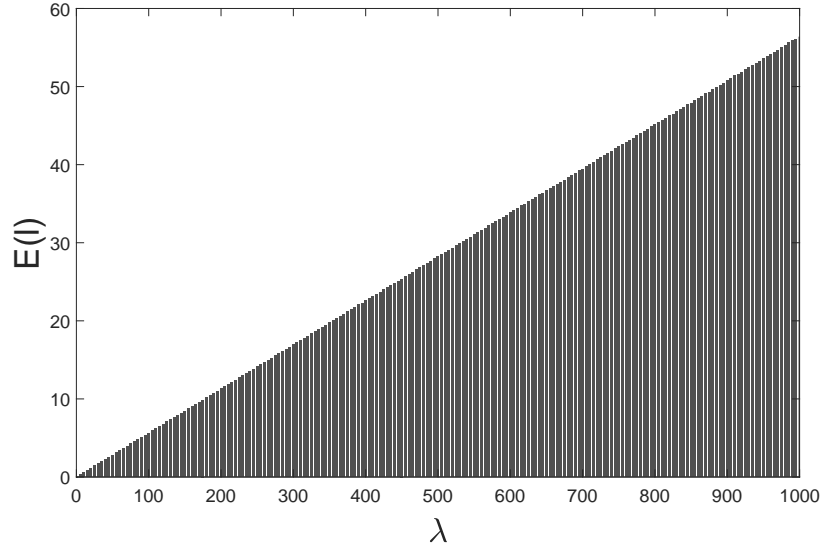
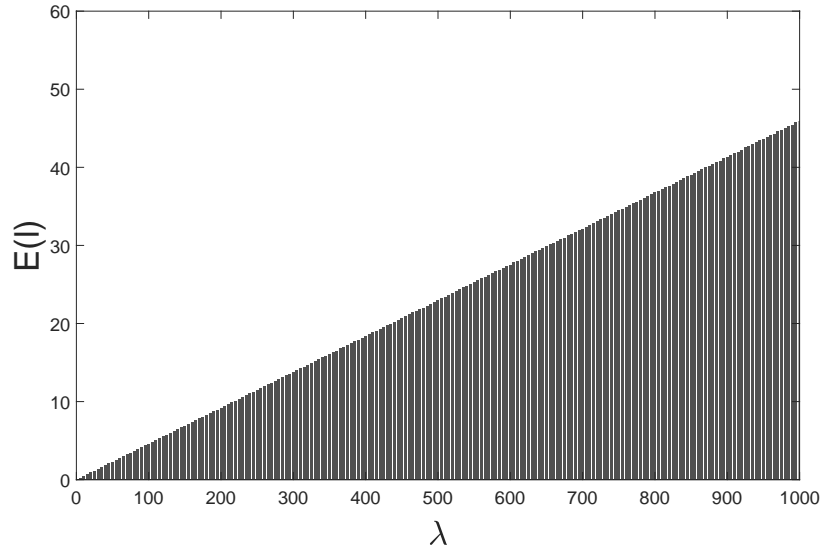


Figure 4: The complexity of the proposed model.



(a) Uniform distribution.



(b) Gaussian distribution.

Figure 5: Expected load for various  $\lambda$  values.

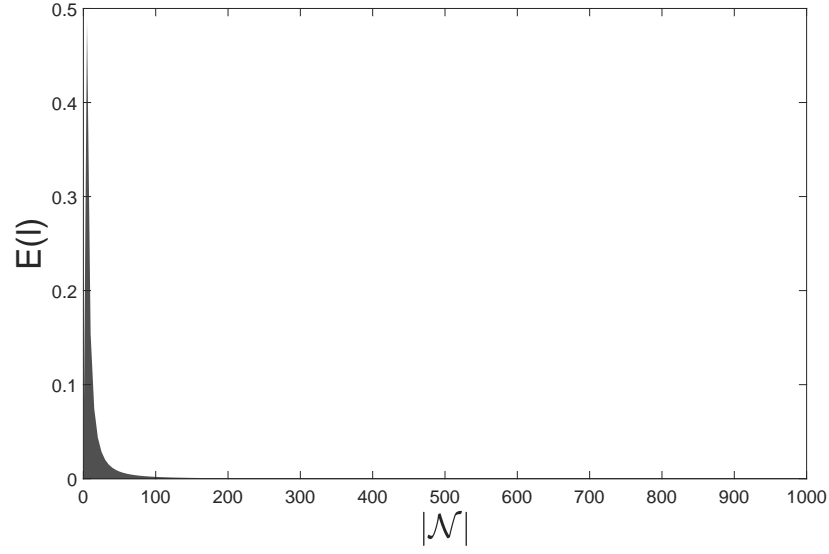
833 is limited. This is more intense when  $|\mathcal{N}| \rightarrow 1,000$ , thus, tasks are offloaded

834 to peer nodes instead of being kept locally. This could lead to a situation  
835 where nodes could execute tasks reported to other nodes instead of keeping  
836 ‘their’ tasks. This is natural as nodes want to offload the incoming tasks and  
837 keep only tasks that are important to be locally executed as indicated by  
838 the adopted classifier. However, such an approach may lead to an exchange  
839 of tasks in the long term, thus, tasks will be continuously circulated in the  
840 network.

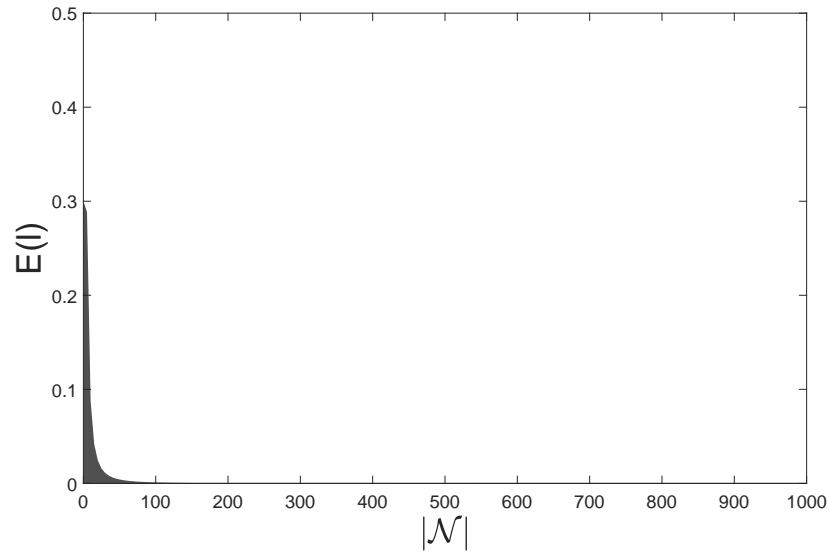
841 The performance of the proposed model for various  $Y$  realizations, is de-  
842 picted in Figure 7. These results are similar as in the previous experimental  
843 scenarios, i.e., the adoption of the Uniform distribution leads to a high  $E(l)$ .  
844 In addition, our results exhibit that when  $Y \leq 10$ , fluctuations in the ex-  
845 pected load can be present. However, such fluctuations are eliminated and  
846 the proposed model exhibits ‘stability’ as  $Y \rightarrow 1,000$ . Again, the adoption  
847 of the Uniform distribution leads to higher expected load compared to the  
848 scenario where the Gaussian distribution is adopted to produce values for  
849 each parameter. Again the observed outcomes can be considered as natural  
850 as the production of values based on the Uniform distribution depicts a very  
851 dynamic environment where nodes’ and tasks’ characteristics are continu-  
852 ously updated. Hence, when a task is generated and reported to a node,  
853 peers’ characteristics may be completely different compared to the previous  
854 execution round. For instance, the Uniform distribution can ‘generate’ a low  
855 value at timestep  $t$  while at  $t + 1$  a high value can be the case. This way,  
856 it is natural to observe higher values for the load compared to the scenario  
857 where the Gaussian distribution is adopted. The reason is that in the Uni-  
858 form distribution scenario, the load is not gathered around the mean but it  
859 is produced in the entire interval in consecutive decision rounds.

860 In Figure 8, we plot the nodes’ expected load vs the rate  $\lambda$  and  $|\mathcal{N}|$ . In  
861 this set of simulations, we experiment with  $p \in \{0.2, 0.8\}$ . When  $p = 0.2$ ,  
862 each node will locally execute the 20% of the incoming tasks while  $p = 0.8$   
863 indicates that nodes will locally execute the 80% of the incoming tasks. The  
864 expected load ‘follows’ the probability  $p$ , i.e., a low  $p$  leads to a low expected  
865 load. This is natural, however, it is interesting to observe that, no matter  
866  $p$ , when the number of nodes is high, the expected load for each node will  
867 be minimized. These outcomes confirm our expectations for the load of the  
868 nodes when tasks arrive at high rates.

869 In Figure 9, we present our results for the long term expected for each  
870 node. In this set of experiments, we consider that the success probability  
871 for peers is around 0.5. We observe that the expected load, in the lifetime



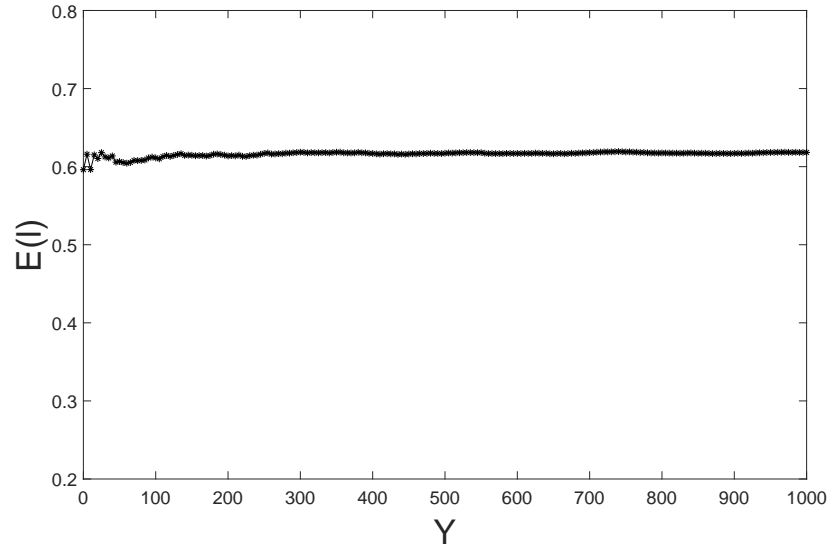
(a) Uniform distribution.



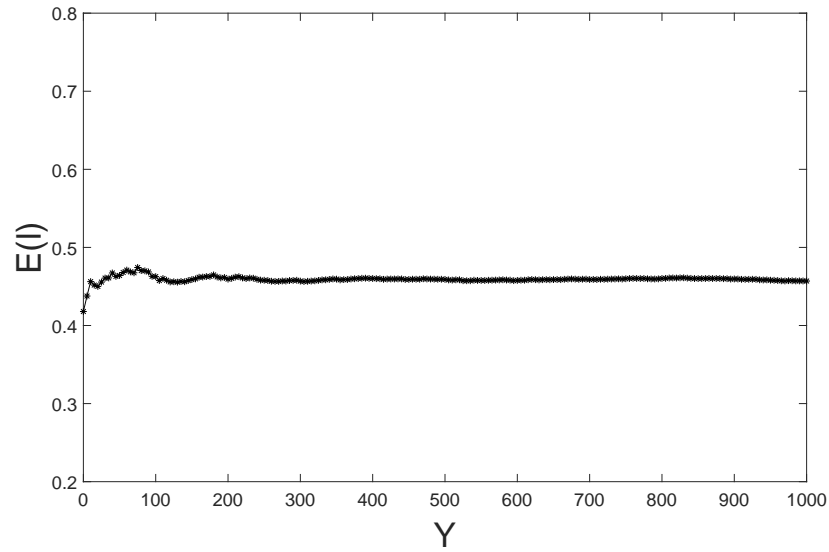
(b) Gaussian distribution.

Figure 6: Short term expected load for various  $|\mathcal{N}|$  values.

872 of the network, is low except the scenarios where the number of nodes is



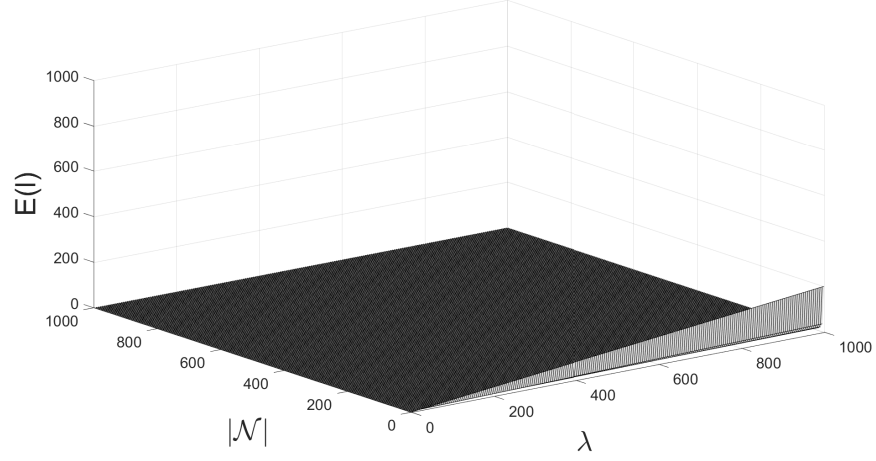
(a) Uniform distribution.



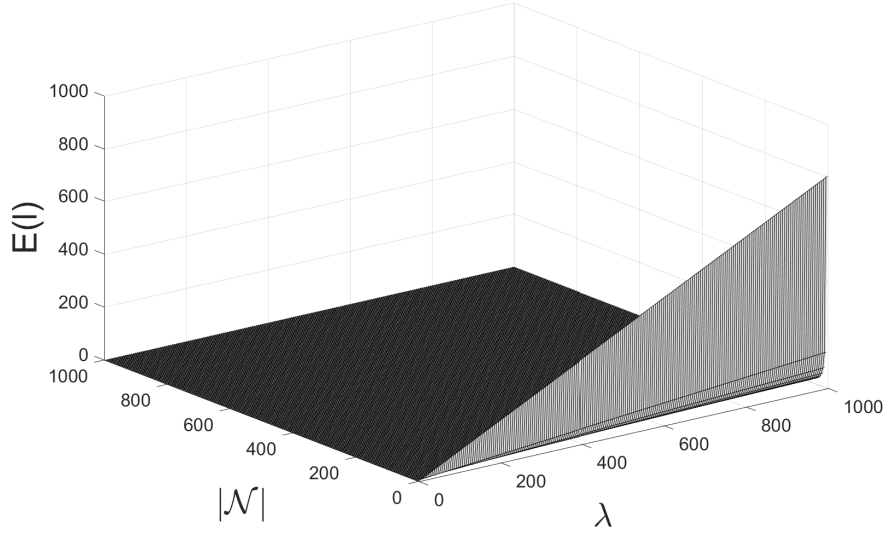
(b) Gaussian distribution.

Figure 7: Short term expected load vs different TRT cardinality.

873 limited and the local probability of success is high (close to unity). These



(a)  $p=0.2$ .



(b)  $p=0.8$ .

Figure 8: Short term expected load vs the probability of local execution.

874 experiments enhance our view that when  $|\mathcal{N}|$  is high, the incoming tasks  
875 could be served, in total, by the network without the need of transferring  
876 tasks to the Fog/Cloud. When we have a high number of nodes present in  
877 the network, we secure the execution of the incoming tasks no matter their



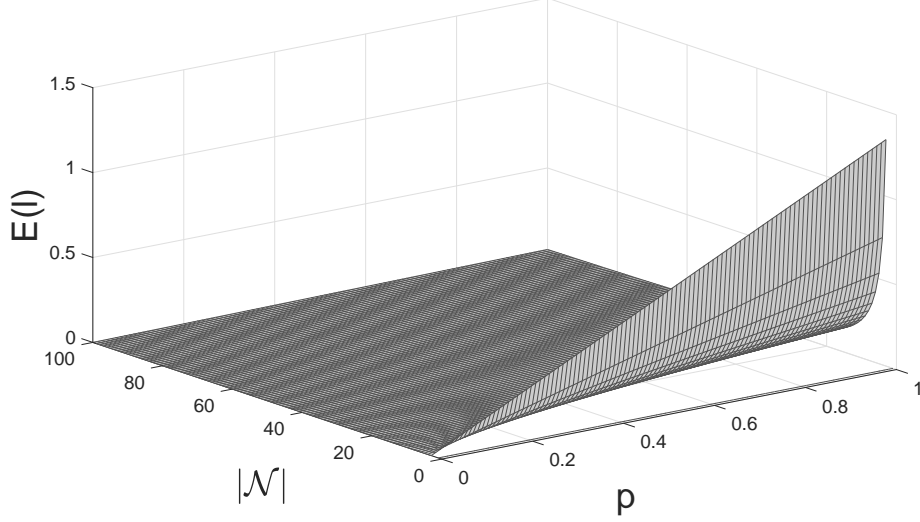


Figure 9: Long term expected load vs  $p$  and  $|\mathcal{N}|$ .

878 characteristics while the load of each node remains at low levels. However, as  
 879 already mentioned, we should take into consideration the burden for trans-  
 880 ferring tasks in the network compared to the latency that we will enjoy if  
 881 tasks should be allocated to the Fog/Cloud. In addition, these results depict  
 882 the load for receiving tasks in a time unit (e.g., second, hour, day, week), i.e.,  
 883 an ‘execution era’. This means that we can easily support multiple groups  
 884 of tasks, thus, multiple ‘execution eras’ as the load will be also limited.

885 In our simulations, the  $k$ NNC exhibits high performance as it results  
 886  $\epsilon = 1.0$ . This means that no false positive events are identified, thus, the  
 887 corresponding tasks are correctly transferred to the network. In addition, we  
 888 observe  $\zeta = 0.97$  which means that false negatives events are also limited. For  
 889 the remaining metrics, we get  $\phi = 0.98$  and  $\psi = 0.98$ . These results expose  
 890 the accuracy of our model in the identification of the tasks that should be  
 891 locally executed.

892 We also evaluate our scheme in the peer selection process. We want to  
 893 identify if the characteristics of the selected peer are those that facilitate the  
 894 execution of the allocated task. For this, we deliver the mean values for each  
 895 parameter calculated over a high number of experiments. In Fig. 10, we  
 896 present our results for  $l$  and for each experimental scenario. We observe that  
 897 the lowest load is achieved in Scenario B. In this scenario, the weight of the

utility for load is the highest among the available weights, thus, the proposed scheme naturally pays more attention on the load of the peer where every task will be allocated. Recall that weights are adopted in the calculation of the utility in the additive utility function. We also observe that the higher the number of nodes, the lower the load of the selected peer becomes confirming again the above discussed outcomes. On the other hand, in Scenarios C & D, we observe the highest average load, i.e., in scenarios where  $l$  is assigned with a low weight compared to the remaining parameters. The mean  $l$  is below 0.4 when  $|\mathcal{N}| \rightarrow 1,000$ . The increased number of nodes positively affects the final outcome as our scheme has many alternatives for selecting the final peer. The involvement of multiple utility functions (an ensemble scheme) manages to find the appropriate peers when a task should be allocated in the network.

In Fig. 11, we present our results concerning the available resources  $r$  in the selected peer. In the majority of the results  $r$  is above 0.5 while the increased number of nodes assists in the increment of the final outcome. The highest mean  $r$  is observed in Scenarios B and C when  $|\mathcal{N}| = 1,000$ . Our outcomes indicate that the selected nodes are characterized by a high availability of resources that can be devoted to the execution of the allocated tasks. In Fig. 12, we observe our results concerning  $\tau$ . We get the highest outcome in Scenario A when  $|\mathcal{N}| = 100$ . In general, the discussed results are judged as efficient due to that  $\tau$  is close or over 0.6 for the majority of the cases. Our experimental evaluation for  $\kappa$  is presented in Fig. 13. We observe that the lowest value is related to Scenario D where we assign the highest weight for  $\kappa$ . Outcomes show that the increased weight and the increased number of nodes assist our scheme to select a peer with a low communication cost. One can observe that, in the majority of the experimental scenarios,  $\kappa$  is below 0.4 while it is approaching 0.2 when  $|\mathcal{N}| \rightarrow 1,000$ . The high number of nodes present in the network gives more opportunities to find the lowest possible communication cost, thus, it minimizes the communication overhead of the network. This way, we can limit the resources and the time required to allocate tasks and get the final response.

We devote a set of experiments to reveal the allocation of the ‘rejected’ tasks to the appropriate peer. We focus on the multi-attribute optimality, meaning that the proposed scheme takes into consideration all the parameters at the same time. In Table 2, we present our results for the Scenarios A and B. We observe that the difference of the selected peer (as resulted by our model) with the peer exhibiting the lowest load is around 0.420 and 0.270

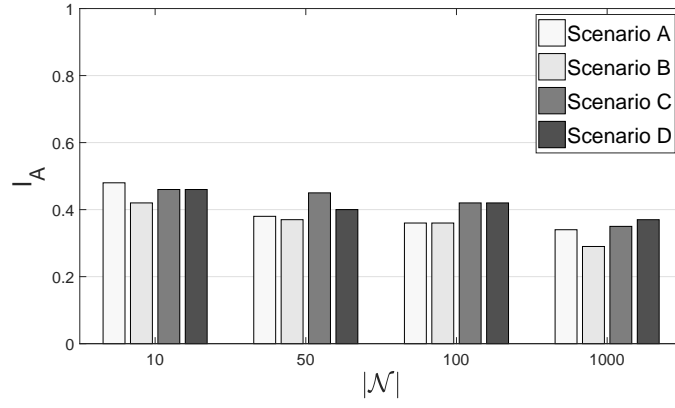


Figure 10: Our results for the mean load of the selected peers.

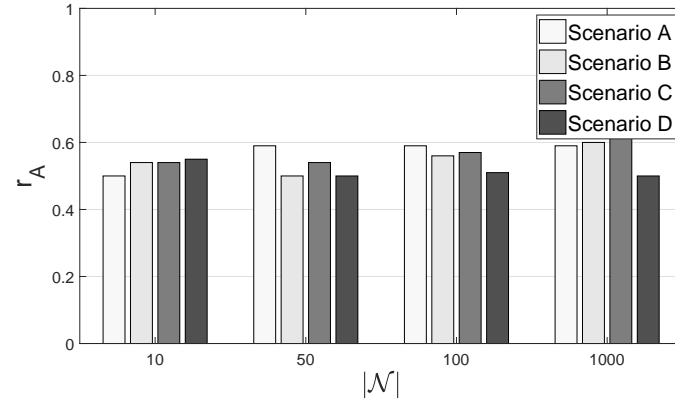


Figure 11: Our results for the mean resources of the selected peers.

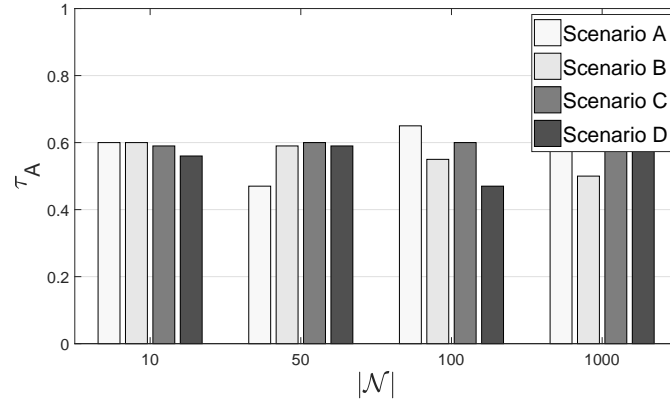


Figure 12: Our results for the mean speed of the selected peers.

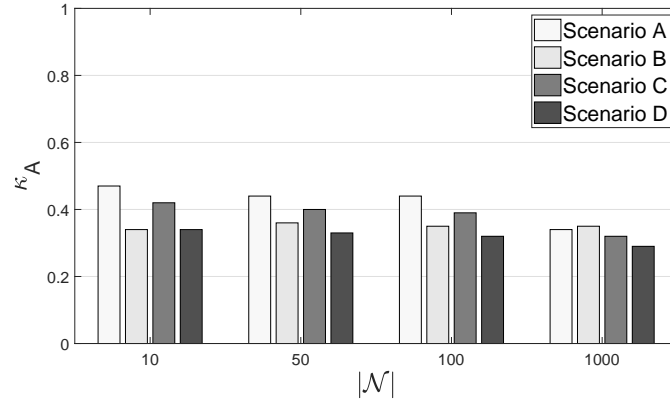


Figure 13: Our results for the mean cost of the selected peers.

936 for Scenarios A and B, respectively. Recall that in Scenario B, the weight  
 937 of the load is the highest when calculating the final utility. We observe  
 938 that the increased weight leads to the selection of a peer that is close to  
 939 the optimal decision. In any case, decisions under the Scenario B lead to  
 940 better results for  $l$  compared to the decisions made under the Scenario A.  
 941 Our model manages to select a peer that exhibits ‘better’ characteristics  
 942 for the remaining parameters in the majority of the experimental scenarios.  
 943 This is depicted by the negative values, i.e., the selected peer exhibits higher  
 944 resources, speed and lower cost than the peer with the lowest load in the  
 945 network. Similar results we get if we focus on Scenarios C and D (see Table 3).  
 946 These outcomes support the observation that our model can be adopted to  
 947 select peers exhibiting the best possible characteristics under the perspective  
 948 of having a multi-attribute decision making.

Table 2: Optimality results for Scenarios A & B (synthetic trace).

$ \mathcal{N} $	Scenario A				Scenario B			
	$l_B$	$r_B$	$\tau_B$	$\kappa_B$	$l_B$	$r_B$	$\tau_B$	$\kappa_B$
10	0.420	-0.125	-0.123	-0.112	0.270	-0.036	-0.016	-0.120
50	0.350	-0.120	0.060	-0.220	0.310	-0.220	-0.150	0.004
100	0.380	-0.090	-0.200	-0.106	0.290	0.090	-0.230	-0.080
1,000	0.310	-0.020	-0.040	-0.030	0.290	-0.059	-0.096	-0.370

Table 3: Optimality results for Scenarios C & D (synthetic trace).

$ \mathcal{N} $	Scenario C				Scenario D			
	$l_B$	$r_B$	$\tau_B$	$\kappa_B$	$l_B$	$r_B$	$\tau_B$	$\kappa_B$
10	0.290	0.029	-0.010	-0.109	0.350	0.040	0.120	-0.140
50	0.350	-0.114	-0.010	-0.196	0.370	-0.100	0.009	-0.001
100	0.420	-0.128	-0.001	-0.146	0.330	-0.085	-0.233	0.036
1,000	0.310	-0.060	-0.138	-0.136	0.330	-0.103	-0.045	-0.162

949 We also perform a set of experiments adopting the real dataset. Our  
 950 results deliver  $\epsilon = 0.81$ ,  $\zeta = 0.49$ ,  $\psi = 0.67$ , and  $\phi = 0.61$ . We observe  
 951 that, compared to the synthetic trace, there is an increased number of false  
 952 positives and false negatives. A number of positive events (i.e., the local

953 execution of a task) is not identified, thus, the corresponding tasks are trans-  
 954 ferred to peers. From the 517 tasks, 163 are locally executed while 354 are  
 955 transferred to peer nodes. The interesting is that no task is transferred to  
 956 be executed in Fog/Cloud.

957 We report on the optimality results for the real dataset. Tables 4 and 5  
 958 present our outcomes for Scenario A, Scenario B, Scenario C and Scenario  
 959 D, respectively. In general, the load of the selected nodes is lower than in the  
 960 experiments realized with the synthetic trace. The proposed model manages  
 961 to select nodes that their characteristics are close or lower than the best  
 962 possible node selection. The interesting is that in this set of experiments,  
 963 the number of the nodes present in the network affects our results. One can  
 964 observe an increment for  $l$  or  $\kappa$  as  $|\mathcal{N}| \rightarrow 1,000$ . For Scenario A, the real trace  
 965 exhibits the best performance for  $l$  and  $\kappa$  while for the remaining metrics the  
 966 best performance is achieved through the adoption of the synthetic trace.  
 967 For Scenario B, we observe similar performance in both cases with some  
 968 fluctuations in the results. For Scenario C, the adoption of the real dataset  
 969 leads to the best performance for  $l$  while the adoption of the synthetic trace  
 970 leads to the best performance for  $\kappa$ . Similar performance is observed for  $r$   
 971 and  $\tau$ . Finally, for Scenario D, the synthetic trace leads to the best results  
 972 for  $\tau$  while for the remaining metrics we observe a similar behavior.

Table 4: Optimality results for Scenarios A & B (real dataset).

$ \mathcal{N} $	Scenario A				Scenario B			
	$l_B$	$r_B$	$\tau_B$	$\kappa_B$	$l_B$	$r_B$	$\tau_B$	$\kappa_B$
10	0.205	-0.055	0.091	-0.055	0.174	0.009	0.107	-0.009
50	0.264	0.004	0.043	-0.004	0.209	0.080	-0.065	-0.080
100	0.264	-0.082	-0.088	0.082	0.261	0.020	-0.053	-0.020
1,000	0.287	-0.310	0.004	0.310	0.293	-0.296	0.010	0.296

Table 5: Optimality results for Scenarios C & D (real dataset).

$ \mathcal{N} $	Scenario C				Scenario D			
	$l_B$	$r_B$	$\tau_B$	$\kappa_B$	$l_B$	$r_B$	$\tau_B$	$\kappa_B$
10	0.193	0.084	0.031	-0.084	0.194	0.041	0.079	-0.041
50	0.270	-0.056	0.031	0.056	0.262	0.067	-0.050	-0.067
100	0.257	-0.029	-0.035	0.029	0.272	0.033	0.009	-0.033
1,000	0.269	-0.293	0.007	0.293	0.277	-0.295	0.019	0.295

973 We compare the performance of our model (i.e., the ‘Model’) with the  
 974 scheme presented in [3]. In [3], the authors propose a task scheduling algo-  
 975 rithm (ETSI) for IoT that is based on a heuristic to finalize the allocations  
 976 of tasks to the available nodes. The algorithm adopts a node state analyzer  
 977 that delivers the final outcome based on the remaining energy, the distance  
 978 from the edge of the network and the number of neighbors. The edge gate-  
 979 way calculates the rank of each node and decides on the final allocation for  
 980 each task. Actually, the node with the lowest ranking is selected for the  
 981 final allocation. In Tables 6, and 7, we present our results for Scenario A,  
 982 Scenario B, Scenario C and Scenario D, respectively. As the experimental  
 983 results presented in [3] focus on the network lifetime and load, in our results,  
 984 we consider the outcomes for  $l_B$  and  $r_B$ . We observe that the Model out-  
 985 performs the ETSI for all the experimental scenarios. There is a significant  
 986 difference in the load of the selected node where tasks will be allocated. The  
 987 reason is that ETSI mainly takes into consideration the energy issues and the  
 988 distance of nodes from the gateway without paying significant attention on  
 989 the load. However, the increased load may negatively affect the energy re-  
 990 sources especially when the allocated tasks are characterized by an increased  
 991 complexity.

Table 6: Comparison of the optimality results (Scenarios A & B).

$ \mathcal{N} $	Scenario A				Scenario B			
	Model		ETSI		Model		ETSI	
	$l_B$	$r_B$	$l_B$	$r_B$	$l_B$	$r_B$	$l_B$	$r_B$
100	0.264	-0.082	0.490	0.058	0.261	0.020	0.540	0.017
1,000	0.287	-0.310	0.701	-0.057	0.293	-0.296	0.687	-0.042

Table 7: Comparison of the optimality results (Scenarios C & D).

$ \mathcal{N} $	Scenario C				Scenario D			
	Model		ETSI		Model		ETSI	
	$l_B$	$r_B$	$l_B$	$r_B$	$l_B$	$r_B$	$l_B$	$r_B$
100	0.257	-0.029	0.489	0.064	0.272	0.033	0.501	0.076
1,000	0.269	-0.293	0.710	-0.044	0.277	-0.295	0.698	-0.067

992 Trying to reveal the hidden aspects of the performance of our model, we  
 993 provide plots for the probability density estimation (pde) for each parameter  
 994 in Fig. 14. We set equal weights (i.e., 0.25) for each parameter and record  
 995 their realization. We observe that  $l$  and  $\kappa$  are concentrated in the first half  
 996 of the interval  $[0, 1]$  while  $\tau$  is concentrated at the upper part of the same  
 997 interval.  $r$  is concentrated at the middle of the interval. In any case, these  
 998 results exhibit the potential of the proposed model to select the appropriate  
 999 peer when it is necessary.

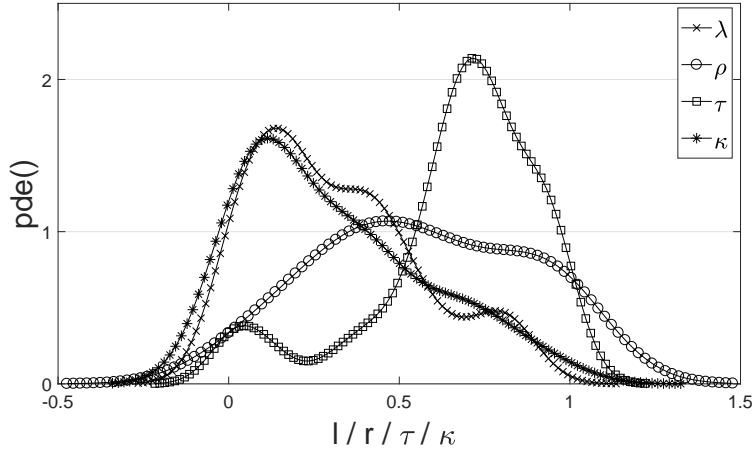


Figure 14: Probability density estimation for the model parameters.

## 1000 7. Conclusions

1001 IoT nodes are capable of collecting and processing various data becoming  
 1002 knowledge providers. Recent advances in the IoT domain involve the exe-  
 1003 cution of processing tasks at the edge, at the nodes, to limit the time for



retrieving results. IoT nodes are characterized by limited computational capabilities while they are instructed to execute multiple tasks. Hence, nodes, when tasks ‘arrive’, should select the tasks that will be executed locally or be transferred to their peers in the network. This way, we create a collaborative, however, distributed scheme for tasks execution trying to find paths for minimizing the response time without jeopardizing the resources of nodes.

We describe a scheme that, in a distributed manner, sequentially decides where the tasks will be processed. Our scheme pushes the task allocation intelligence into the edge network by providing a two-level decision making mechanism. The mechanism derives decisions related to which tasks will be executed locally in the nodes. The proposed decision making scheme sequentially examines possible actions to optimally decide the place where tasks will be executed. Every node autonomously decides the execution of tasks. We evaluate our scheme with synthetic and real data and provide numerical results. We show that the proposed scheme manages to deliver decisions that optimally select the place of the execution based on a set of parameters. When the decision concerns the group of nodes, the proposed scheme selects a node in the network edge and transfers the task there. Our experimental evaluation shows that the selected nodes are appropriate minimizing the average difference with the optimal solution. Our future research plans involve the provision of an uncertainty management model. Such a model could incorporate more easily the uncertainty present in the decision making process.

## Acknowledgment

This work is funded by the EU/H2020 Marie Skłodowska-Curie Action Individual Fellowship (MSCA-IF-2016) under the project INNOVATE (Grant No. 745829).

- [1] Aazam, M., Hung, P. P., Huh, E. N., ‘Smart Gateway based Communication for Cloud of Things’, 9th ICSSNIP, 2014.
- [2] Awadalla, M. H. A., ‘Task Mapping and Scheduling in Wireless Sensor Networks’, Int. Journal of Computer Science, 440(4), 2013.
- [3] Baranidharan, B., Saravanan, K., ‘ETSI: Efficient Task Allocation in Internet of Things’, International Journal of Pure and Applied Mathematics, vol. 117(22), 2017, pp. 229–233.

- 1038 [4] Cortez, P., Morais, A., 'A Data Mining Approach to Predict Forest Fires  
1039 using Meteorological Data', In Proc. of the 13th Portuguese Conference  
1040 on Artificial Intelligence, Guimares, Portugal, 2007, pp. 512–523.
- 1041 [5] De Benedetti, M., Messina, F., Pappalardo, G., Santoro, C., 'JarvSis:  
1042 A Distributed Scheduler for IoT Applications', Cluster Computing, 20,  
1043 2017, pp. 1775–1790.
- 1044 [6] Bharti, S., Pattanaik, K., 'Task Requirement Aware Pre-processing and  
1045 Scheduling for IoT Sensory Environments', Ad Hoc Networks, 50, 2016,  
1046 pp. 102–114.
- 1047 [7] Chen, Z., Hu, W., Wang, J., Zhao, S., Amos, B., Wu, G., Ha, K., El-  
1048 gazzar, K., Pillai, P., Klatzky, R., Siewiorek, D., Satyanarayanan, M.,  
1049 'An Empirical Study of Latency in an Emerging Class of Edge Comput-  
1050 ing Applications for Wearable Cognitive Assistance', in Proc. of the 2nd  
1051 ACM/IEEE Symposium on Edge Computing, 2017.
- 1052 [8] Choi, H., Lim, J. B., Yu, H., Lee, E. Y., 'Task Classification Based  
1053 Energy-Aware Consolidation in Clouds', Scientific Programming, vol.  
1054 2016, 2016.
- 1055 [9] Coltin, B., Veloso, N., 'Mobile Robot Task Allocation in Hybrid Wireless  
1056 Sensors Networks', in 2010 Int. Conf. on Intelligent Robots and Systems,  
1057 2010.
- 1058 [10] Dai, L., Chang, Y., Shen, Z., 'An Optimal Task Scheduling Algorithm  
1059 in Wireless Sensor Networks', Int. JCCC, 1, 2011, pp. 101–112.
- 1060 [11] Dueck, G., Scheuer, T., 'Threshold accepting: A general purpose opti-  
1061 mization algorithm appearing superior to simulated annealing', Journal  
1062 of Computational Physics, vol. 90(1), 1990, pp. 161–175.
- 1063 [12] Edalat, N., Xiao, W., Tham, C.-K., Keikha, E., Ong, L.-L., 'A price-  
1064 based adaptive task allocation for Wireless Sensor Network', 6th IC-  
1065 MASS, 2009.
- 1066 [13] Emerso, P., 'The Original Borda Count and Welfare', Social Choice and  
1067 Welfare, 40(2), 2013, pp. 353–358.

- 1068 [14] Formato, R., 'Dynamic Threshold Optimization - A New Approach?',  
1069 arXiv:1206:0414, 2012.
- 1070 [15] Gaines, B., 'A Situated Classification Solution of a Resource Allocation  
1071 Task Represented in a Visual Language', *International Journal of Human-  
1072 Computer Studies*, vol. 40(2), 1994, pp. 243–271.
- 1073 [16] Garcia Lopez, P., Montresor, A., Epema, D., Datta, A., Higashino, T.,  
1074 Iamnitchi, A., Barcellos, M., Felber, P., Riviere, E., 'Edge-centric Com-  
1075 puting: Vision and Challenges', *ACM SIGCOMM Computer Communi-  
1076 cation Review*, 45(5), 2015.
- 1077 [17] Garmabaki, A. H. S., Ahmadi, A., Ahmadi, M., 'Maintenance Optimiza-  
1078 tion Using Multi-Attribute Utility Theory', *Current Trends in Reliability,  
1079 Availability, Maintainability and Safety*, 2015, pp. 13–25.
- 1080 [18] Gennert, M., Yuille, A., 'Determining the Optimal Weights in Multi-  
1081 ple Objective Function Optimization', in *Proc. of the 2nd International  
1082 Conference on Computer Vision*, 1988.
- 1083 [19] Greenberg, A., Hamilton, J., Maltz, D., Patel, 'The Cost of a Cloud:  
1084 Research Problems in Data Center Networks', *ACM SIGCOMM*, 39(1),  
1085 2008, pp. 68–73.
- 1086 [20] Han, J., Kamber, M., Pei, J., 'Data Mining, Concepts and Techniques',  
1087 Morgan Kaufmann Publishers, 2012.
- 1088 [21] Hershenson, M., Boyd, S., Lee, T., 'GPCAD: a tool for CMOS opamp  
1089 synthesis', in *proc. of IEEE/ACM International Conference on Computer-  
1090 Aided Design*, pp. 296-303, 1998.
- 1091 [22] Hu, X., Xu, B., 'Task Allocation Mechanism Based on Genetic Algo-  
1092 rithm in Wireless Sensor Networks', in *ICAIC*, 2011.
- 1093 [23] Keeney, R. L., Raiffa, H., 'Decisions with multiple objectives: prefer-  
1094 ences and value trade-offs', Cambridge University Press, 1993.
- 1095 [24] Kolomvatsos, K., Loukopoulos, T., 'Scheduling the Execution of Tasks  
1096 at the Edge', *2018 IEEE Conference on Evolving and Adaptive Intelligent  
1097 Systems*, Rhodes, Greece, May 25-27, 2018.

- 1098 [25] Krishnapriya, S., Joby, P. P., 'QoS Aware Resource Scheduling in Inter-  
1099 net of Things-Cloud Environment', Int. JSER, 6(4), 2015.
- 1100 [26] Lam, L., 'Theory and Application of Majority Vote - From Condorcet  
1101 Jury Theorem to Pattern Recognition', 2nd International Conference on  
1102 mathematics education into the 21st century: Mathematics for Living,  
1103 Amman, Jordan, 2000.
- 1104 [27] Liu, J., Mao, Y., Zhang, J., Letaief, K. B., 'Delay-Optimal  
1105 Computation Task Scheduling for Mobile-Edge Computing Systems',  
1106 <https://arxiv.org/abs/1604.07525>, 2016.
- 1107 [28] Morabito, R., 'Virtualization on Internet of Things Edge Devices with  
1108 Container Technologies: A Performance Evaluation', IEEE Access, vol.  
1109 5, 2017, pp. 8835–8850.
- 1110 [29] Morabito, R., Cozzolino, V., Yi Ding, A., Beijar, N., Ott, J., 'Consol-  
1111 idate IoT Edge Computing with Lightweight Virtualization', IEEE Net-  
1112 work, 2018.
- 1113 [30] Moschakis, I., Karatza, H., 'Towards Scheduling for Internet-of-Things  
1114 Applications on Clouds: A Simulated Annealing Approach', Concurrency  
1115 and Computation, Combined Special Issues on the Internet of Things,  
1116 27(8), 2015, pp. 1886–1899.
- 1117 [31] Narula, S., 'Hierarchical location-allocation problems: A classification  
1118 scheme', European Journal of Operational Research, vol. 15(1), 1984,  
1119 93-99.
- 1120 [32] Nelson, R., 'Probability, Stochastic Processes, and Queueing Theory',  
1121 Springer-Verlag, New York, 1995.
- 1122 [33] Pahl, C., Helmer, S., Miori, L., Sanin, J., Lee, B., 'A Container-Based  
1123 Edge Cloud PaaS Architecture Based on Raspberry Pi Clusters', in proc.  
1124 of the 4th IEEE International Conference on Future Internet of Things  
1125 and Cloud Workshops, Vienna, Austria, 2016.
- 1126 [34] Pahl, C., Lee, B., 'Containers and Clusters for Edge Cloud Architectures  
1127 - a Technology Review', in proc. of the 3rd International Conference on  
1128 Future Internet of Things and Cloud, 2015.

- 1129 [35] Pasteris, S., Wang, S., Makya, C., Chan, K., Herbster, M., 'Data Dis-  
1130 tribution and Scheduling for Distributed Analytics Tasks', IEEE SWC  
1131 Conference, 2017.
- 1132 [36] Prince, A., Smolensky, P., 'Optimality Theory: Constraint Interaction  
1133 in Generative Grammar', y, 2008.
- 1134 [37] Razavinegad, A., 'Task Allocation In Robot Mobile Wireless Sensor Net-  
1135 works', Int. Journal of Scientific & Technology Research, 3(6), 2014.
- 1136 [38] Roman, R., Lopez, J., Mambo, M., 'Mobile edge computing, Fog et  
1137 al.: A survey and analysis of security threats and challenges', Future  
1138 Generation Systems, 78(2), 2018, pp. 680–698.
- 1139 [39] Santos, J., Wauters, T., Volckaert, B., De truck, F., 'Fog Computing:  
1140 Enabling the Management and Orchestration of Smart City Applications  
1141 in 5G Networks', Entropy, vol. 4, 2018.
- 1142 [40] Satyanarayanan, M., 'A brief history of cloud offload: A personal jour-  
1143 ney from Odyssey through cyber foraging to cloudlets', Mobile Comput-  
1144 ing Communications, 18(4), 2015, pp. 19–23.
- 1145 [41] Shanthan, B.J., Kumar, A. D. V., Govindrajan, E., Arockian, L.,  
1146 'Scheduling for Internet of Things Applications on Cloud: A Review',  
1147 Imperial Journal of Interdisciplinary Research, 3(1), 2017.
- 1148 [42] Silberschatz, A., Baer Galvin, P., Gagne, G., 'Operating Systems Con-  
1149 cepts', 9th Ed., Wiley, 2013.
- 1150 [43] Soorapanth, T., 'Understanding and Optimizing Weight Factors in  
1151 Multi-Objective Geometric Programming', in proc. of the ECTI Inter-  
1152 national Conference on Electrical Engineering/Electronics, Computer,  
1153 Telecommunications and Information Technology, 2010.
- 1154 [44] Soorapanth, T., 'Gaining insights in analog design via Geometric Pro-  
1155 gramming', in proc. of the International Symposium on Communications  
1156 and Information Technologies, pp. 121-126, 2007.
- 1157 [45] Soylu, B., Kapan Ulusoy, S., 'A preference ordered classification for a  
1158 multi-objective max-min redundancy allocation problem', Computers and  
1159 Operations Research, vol. 38(12), 2011, pp. 1855–1866.

- 1160 [46] Sun, G., Li, Y., Liao, D., Chang, V., 'Law-Latency Orchestration for  
1161 Workflow-Oriented Service Function Chain in Edge Computing', *Future*  
1162 *Generation Computer Systems*, vol. 85, 2018, pp. 116–128.
- 1163 [47] Sun, J., Sun, S., Li, K., Liao, D., Sangaiah, A. K., Chang, V., 'Efficient  
1164 Algorithm for Traffic Engineering in Cloud-of-Things and Edge Comput-  
1165 ing', *Computers and Electrical Engineering*, vol. 69, 2018, pp. 610–627.
- 1166 [48] Tian, Y., Ekici, E., Ozguner, F., 'Energy-Constrained Task Mapping  
1167 and Scheduling in Wireless Sensor Networks', *IEEE ICMAS*, 2005.
- 1168 [49] Varshney, P., 'Distributed Detection and Data Fusion', Springer, 1997.
- 1169 [50] Voigt, T., Fried, R., Backes, M., Rhode, W., 'Threshold optimization for  
1170 classification in imbalanced data in a problem of gamma-ray astronomy',  
1171 *Advances in Data Analysis and Classification*, vol. 8(2), 2014, pp. 195–  
1172 216.
- 1173 [51] Voinescu, A., Tudose, D. S., Tapus, N., 'Task Scheduling in Wireless  
1174 Sensor Networks', 6th ICNS, 2010.
- 1175 [52] Weiss, S., Arne Schwarz, J., Stolletz, R., 'The Buffer Allocation  
1176 Problem: A Joint Classification and Review of Decision Problems,  
1177 Solution Approaches, and Test Instances', *SSRN Electronic Journal*,  
1178 10.2139/ssrn.2843435.
- 1179 [53] Wu, G., Bao, W., Zhang, X., 'A General Cross-Layer Cloud Scheduling  
1180 Framework for Multiple IoT Computer Tasks', *Sensors*, vol. 18, 2018.
- 1181 [54] Xu, J., Palanisamy, B., Ludwig, H., Wang, Q., 'Zenith: Utility-Aware  
1182 Resource Allocation for Edge Computing', *IEEE Edge*, 2017.
- 1183 [55] Yang, J., Zhang, H., Ling, Y., Pan, C., Sun, W., 'Task Allocation for  
1184 Wireless Sensor Network Using Modified Binary Particle Swarm Opti-  
1185 mization', *IEEE Sensors Journal*, 14(3), 2014, pp. 882–892.
- 1186 [56] Yang, J., 'Complexity Analysis of New Task Allocation Problem Using  
1187 Network Flow Method on Multicore Clusters', *Mathematical Problems*  
1188 *in Engineering*, art. id 723497, 2014.

- 1189 [57] Yu, Y., Prasanna, V., 'Energy-Balanced Task Allocation for Collab-  
1190 orative Processing in Wireless Sensor Networks', Mobile Networks and  
1191 Applications, 10(1-2), 2005, pp. 115–131.
- 1192 [58] Zhang, Q., Zhani, M. F., Boutaba, R., Hellerstein, J. L., 'Dynamic  
1193 Heterogeneity-Aware Resource Provisioning in the Cloud', IEEE Trans-  
1194 actions on Industrial Informatics, 2(1), 2014.